HHS Public Access

Author manuscript

Annu Rev Biomed Eng. Author manuscript; available in PMC 2015 June 01.

Published in final edited form as:

Annu Rev Biomed Eng. 2014 July 11; 16: 505–532. doi:10.1146/annurev-bioeng-071813-104908.

Mechanosensing at the Vascular Interface

John M. Tarbell[1], **Scott I. Simon**[2], and **Fitz-Roy E. Curry**[2,3]

Scott I. Simon: sisimon@ucdavis.edu

[1]Department of Biomedical Engineering, The City College of the City University of New York, New York, NY 10031

[2]Department of Biomedical Engineering, University of California, Davis, California 95616

[3]Department of Physiology and Membrane Biology, University of California, Davis, California 95616

Abstract

Mammals are endowed with a complex set of mechanisms that sense mechanical forces imparted by blood flow to endothelial cells (ECs), smooth muscle cells, and circulating blood cells to elicit biochemical responses through a process referred to as mechanotransduction. These biochemical responses are critical for a host of other responses, including regulation of blood pressure, control of vascular permeability for maintaining adequate perfusion of tissues, and control of leukocyte recruitment during immunosurveillance and inflammation. This review focuses on the role of the endothelial surface proteoglycan/glycoprotein layer—the glycocalyx (GCX)—that lines all blood vessel walls and is an agent in mechanotransduction and the modulation of blood cell interactions with the EC surface. We first discuss the biochemical composition and ultrastructure of the GCX, highlighting recent developments that reveal gaps in our understanding of the relationship between composition and spatial organization. We then consider the roles of the GCX in mechanotransduction and in vascular permeability control and review the prominent interaction of plasma borne sphingosine-1 phosphate (S1P), which has been shown to regulate both the composition of the GCX and the endothelial junctions. Finally, we consider the association of GCX degradation with inflammation and vascular disease and end with a final section on future research directions.

Keywords

glycoprotein; proteoglycan; glycocalyx; shear stress; red cell; white cell; vascular permeability; vascular disease; endothelium; sphingosine-1 phosphate

DISCLOSURE STATEMENT

The authors are not aware of any affiliations, memberships, funding, or financial holdings that might be perceived as affecting the objectivity of this review.

INTRODUCTION

In the lifelong quest to maintain vascular homeostasis, mammals are endowed with a complex set of mechanisms to sense mechanical forces imparted by blood flow to endothelial cells (ECs), smooth muscle cells, and circulating blood cells to elicit biochemical responses through a process referred to as mechanotransduction. These responses are critical for regulation of blood pressure, to control vascular permeability for maintaining adequate perfusion of tissues and to control leukocyte recruitment during immunosurveillance and inflammation. Shear stress acting on ECs elicits a myriad of cellular responses that include elongation and alignment of cells in the flow direction (1); enhanced or suppressed production of molecules associated with homeostasis, such as nitric oxide (2), prostacyclin (3), and calcium (4); and gene expression (5). Although the intracellular signaling pathways that mediate these changes have been studied in detail, the cellular structures that sense and transduce shear forces are not as well established. Both transmembrane and intracellular mechanosensors have been reported, including plasma membrane phospholipids, ion channels, receptor tyrosine kinases, G protein–coupled receptors, caveolae, platelet endothelial cell adhesion molecule-1 (PECAM-1) and its associated intercellular junction complex, integrins and their basal adhesion complex, and the endothelial surface glycocalyx (reviewed in 6, 7). Thus, mechanotransduction involves the sensing of shear force at the luminal membrane, as well as at remote sites that mediate cell–cell or cell–matrix anchoring via propagation of forces through the cytoskeleton (7, 8).

A particular focus of this review is on the role of the endothelial surface proteoglycan/glycoprotein layer—the glycocalyx (GCX)—that lines all blood vessel walls (Figure 1) in mechanotransduction and the modulation of blood cell interactions with the EC surface. Although the structure and function of the GCX as a mechanosensor and as part of the vascular permeability barrier have been described in several recent reviews (9–11), particular emphasis in this review is given to recent developments that indicate that the compositions of both the GCX and the intercellular junctions are regulated by the soluble mediator sphingosine-1 phosphate (S1P). S1P is a sphingolipid that is synthesized and carried by red blood cells (RBC) and delivered to the EC surface by plasma proteins, most notably albumin and high-density lipoprotein (HDL). Recent observations show that, although it is not part of the GCX, S1P acting via the S1P receptor 1 (S1P1) on the EC surface not only strengthens the endothelial junctions by stabilizing the EC cytoskeleton but also directly regulates the amount of key components of the GCX present on the endothelial surface. The finding that the stability of the GCX is determined at least in part by maintaining a sufficient concentration of plasma phospholipid S1P raises concerns that the GCX structure may be compromised under many experimental conditions where the local concentration of S1P is maintained at artificially low levels. Furthermore, recent observations that the selective removal of known components of the GCX does not modify standard measures of GCX thickness indicate either that GCX components do not interact as closely as previously assumed or that common measures of GCX thickness are poor indicators of its function. It follows that detailed knowledge of GCX composition alone does not translate directly into an understanding of its functions. In the following sections, we first expand discussion of the biochemical composition and ultrastructure of the GCX,

highlighting recent developments that reveal gaps in our understanding of the relationship between composition and spatial organization. We then consider in detail the roles of the GCX in mechanotransduction and in vascular permeability control and explore the prominent role of plasma-borne S1P in controlling the state of the GCX and the intercellular junction/cytoskeleton. We discuss the association of GCX degradation with inflammation and vascular disease and complete the review with a final section on future research directions.

BIOCHEMICAL COMPOSITION AND ORGANIZATION OF THE GLYCOCALYX

The surface of ECs is covered with many membrane-bound macromolecules, which constitute the GCX. A diagram that integrates many of the components of the GCX is shown in Figure 2, which is adapted from a detailed review (11). Major components of the GCX are glycoproteins bearing acidic oligosaccharides and terminal sialic acids (SA), and proteoglycans (PGs) with their associated glycosaminoglycan (GAG) side chains. GAGs are characterized by distinct disaccharide unit repeats that give rise to different components such as heparan sulfate (HS), chondroitin sulfate (CS), and hyaluronic acid (HA) commonly associated with ECs. HS and CS chains vary between 50 and 150 disaccharide units and have an average molecular weight of about 30 kDa. A GAG chain that is fully extended has an estimated length of about 1 nm per disaccharide unit (12, 13). HS is the most prominent GAG on the surface of ECs and accounts for 50–90% of the total GAG pool, the rest being composed of CS and HA (14). PGs are proteins that contain specific sites where sulfated GAGs are covalently attached (15). The transmembrane syndecans and membrane-bound glypicans are among the three major protein core families of heparan sulfate proteoglycans (HSPGs) found on ECs (along with the basement matrix associated perlecans) (16). From the syndecan family of core proteins, syndecans-1 (33 kDa), -2 (22 kDa), and -4 (22 kDa) are expressed on ECs. They have three GAG attachment sites close to their N-terminus substituted primarily but not exclusively by HS (16, 17). Syndecan-1 contains two additional sites closer to the membrane, reserved for CS (18). Their cytoplasmic tails associate with the cytoskeleton and assist in its organization (19, 20). Glypican-1 (64 kDa) is the only glypican expressed on ECs (16). Its three to four GAG attachment sites are exclusively substituted with HS (21).

Glypican-1 is bound directly to the plasma membrane through a C-terminal glycosylphosphatidylinositol (GPI) anchor (21). The GPI anchor localizes this proteoglycan to lipid rafts, which are cholesterol- and sphingolipid-rich membranous domains involved in vesicular transport and cell signaling (21, 22). Caveolae can be considered a subset of lipid rafts that arise from the incorporation of the protein caveolin-1, a cholesterol carrier, into the membrane, where they may form characteristic cave-like structures (~100 nm) that are supported by the cytoskeleton (23).

In contrast to CS and HS, HA is a much longer disaccharide polymer, of the order of 1,000 to 10,000 kDa, which is synthesized on the cell surface and is not covalently attached to a core protein (24). It is not sulfated but obtains its negative charge from carboxyl groups that endow it with exceptional hydration properties. HA associates with the GCX through its

interaction with surface HA receptors, such as the transmembrane glycoprotein CD44, and CS chains (25).

Until recently, it was widely believed that the structural stability of the GCX depended upon the electrostatic interaction among all of its components and that the degradation of any one component would lead to a collapsed structure (11). Zeng and colleagues (26) recently reported that the nearly complete removal of an individual GAG component (HS, CS, or HA) by a highly selective enzyme had no effect on the thickness or coverage of the remaining components, suggesting that GAG components do not interact strongly with one another.

The association of GAGs with proteins also impacts their structure. Previous studies suggested that the negative charges on GAGs interacted with positively charged arginine residues on albumin to provide a stabilizing electrostatic interaction that was disrupted when protein was removed, leading to a collapse of the overall structure (27). It is known that albumin and other serum components (notably HDL) carry S1P, and it is actually S1P that mediates the aforementioned albumin effect (28, 29). When albumin-bound S1P is removed from the media and S1P1 is vacated, matrix metalloproteinases (MMPs), in particular MMP-9 and MMP-13, are activated, leading to the cleavage of the syndecan-1 ectodomain and the loss of its associated GAGs. When protein (S1P) is reintroduced into the media, reextending the GCX requires new synthesis, which takes hours. This has important implications for experiments that use serum-free media to pacify cells, as an important mechanosensor (the GCX) is lost irreversibly (29).

Completing the picture, glycoproteins with short, branched oligosaccharides attached to their core are also found on the surface of ECs. Many important receptors on the cell surface that contribute to leukocyte adhesion during inflammation, including E-selectin and P-selectin, integrins, and members of the immunoglobulin superfamily such as intercellular adhesion molecule 1 (ICAM-1) and vascular cell adhesion molecule 1 (VCAM-1), have oligosaccharides attached to them and are classified as glycoproteins (12).

Shear stress has a direct effect on synthesis of GCX components. Giantsos-Adams et al. (30), using cultured ECs, showed that after enzymatic removal of HS, shear stress enhanced HS synthesis 1.4-fold compared with static controls. HS was restored on the EC surface within 12 h under flow conditions, compared with 20 h under static conditions (30). Koo et al. (31), working with cultured ECs, found that HS expression was increased and evenly distributed on the apical surface of ECs exposed to an atheroprotective shear waveform (one with a relatively high mean shear and no shear reversal), whereas it was irregularly present on cells exposed to an atheroprone waveform (low mean shear and significant shear reversal). These findings are consistent with observations in the carotid arteries of mice, which showed greater GCX thickness and coverage in the lesion-protected common carotid artery than in the lesion-prone bifurcation region (32).

The role of agents such as S1P that regulate the composition of the GCX and the activity of MMPs is an area of intense investigation. It remains to be determined how the established picture in Figure 2 will be modified as new experiments are designed and carried out that

evaluate the relative abundance of GCX components and their distribution on the EC surface in the presence of physiological levels of S1P.

ULTRASTRUCTURE OF THE GLYCOCALYX

The functions of the GCX depend on the way the chemical components described above are organized into the three-dimensional (3D) structure on the EC surface. The most well-investigated index of GCX structure is the thickness of the layer extending beyond the surface. Table 1 shows representative values of GCX thickness from a variety of techniques ranging from conventional electron microscopy (EM) with additional labeling using electron dense dyes to more recent optical methods on intact vessels. Estimates of GCX thickness span over many orders of magnitude, from tens of nanometers to 10 μm. Figure 3 illustrates the use of some of these methods on bovine aortic endothelial cells (BAECs), with images from conventional EM fixation as well as those using rapid freezing techniques. Ebong and colleagues (33) were the first to apply rapid freezing and cryo-EM to cultured ECs [BAECs and rat fat pad endothelial cells (RFPECs)] in order to avoid the dehydration artifacts of conventional EM. The GCX thickness in transmission electron microscopy (TEM) images prepared with ruthenium red and conventional alcohol dehydration was 42 nm, whereas the cryo-EM thickness was 5.8 μm (RFPECs) and 11.3 μm (BAECs). In between these values are estimates (50–100 nm) based on fluorocarbon-glutaraldehyde fixation (34) and those (220–500 nm) measured on rat myocardial vessels using a similar approach with Alcian blue staining (Table 1).

The experiments described above imaged cells under stationary conditions without flow. The first method to estimate GCX thickness (in the range of 0.4 to 0.5 μm) under flow conditions without fixation used a 70-kDa dextran plasma tracer that was sterically excluded by the GCX (35). To overcome optical difficulties that limit the application of the above method to vessels measuring 12–15 μm in diameter, a new method (see 25 for review), based on high-resolution, near-wall intravital fluorescent microparticle image velocimetry (μ-PIV), was developed to quantify the velocity profile near the vessel wall in postcapillary venules of the mouse cremaster muscle (36). The technique was elaborated in later studies (37, 38). Ultimately, these methods led to estimates of a GCX thickness of 0.5 μm in a 20–40 μm thick mouse cremaster venule on live cells (unfixed) in a physiological flow field.

Several new approaches to GCX imaging based on the use of confocal and multiphoton laser scanning microscopy have been developed. Barker and colleagues (39) used fluorescein isothiocyanate (FITC)-linked wheat germ agglutinin to detect SA on the surface of human umbilical vein endothelial cells (HUVECs) using Z-scans at intervals of 0.5 μm. The GCX thickness of these live cells in vitro, imaged under stationary conditions, was deduced to be 2.5 μm. Stevens and colleagues (40) applied confocal laser scanning microscopy and fluorescence correlation spectroscopy to live bovine lung microvascular endothelial cells (BLMVECs) labeled for both HS and HA, estimating a GCX thickness of 2 to 3 μm. Zeng and colleagues (26) applied a similar technique to RFPECs and observed HS, CS, and HA layers of 2–3-μm thickness. Zeng and colleagues also observed a variation of thickness over the surface with the greatest thicknesses arising in the intercellular junction regions.

Using high-resolution confocal microscopy and in situ/in vivo single microvessel and ex vivo aorta immunostaining, Yen and colleagues (41) found that the thickness of the HS layer on rat mesenteric and mouse cremaster capillaries and postcapillary venules is 1–1.5 μm. Surprisingly, there was no detectable GCX in arterioles using fluorescently labeled anti-HS. The HS thickness was 2–2.5 μm on rat and mouse aorta. The authors also observed that the GCX is continuously and evenly distributed on the aortic wall but not on the microvessel wall where there were large variations in coverage when viewed over a length scale of ~100 μm. Two other groups (42, 43) applied a sidestream dark-field imaging technique to determine the erythrocyte–endothelial gap in sublingual microvessels (5–25 μm diameter) of humans and observed GCX thicknesses in the range of 0.78 to 2.35 μm. When similar methods were applied to human retinal vessels (90 μm and above), a GCX thickness as great as 8.9 μm was observed. Application of these new methods has revealed a much thicker GCX in large blood vessels: 4.3–4.5 μm in the mouse common carotid artery (44, 45), 2.2 μm in the mouse internal carotid artery (46), and 2.5 μm in the external carotid artery (45).

Analysis of the various methods of ultrastructural determination indicates that conventional EM suffers from severe dehydration artifacts producing GCX thickness estimates on the order of 50 nm. When dehydration is avoided using cryo-EM, estimates are 100-fold higher (5–11 μm). Confocal and multiphoton laser scanning microscopy methods provide thickness estimates of the same order of magnitude as those of cryo-EM (1–5 μm). Live imaging of cells under flow conditions using tracer exclusion and erythrocyte–endothelial exclusion layer estimates reveal thicknesses of 0.5 to 2 μm in microvessels and up to 9 μm in larger vessels. Nevertheless, these larger values may also result from artifacts that are not fully understood. For example, a recent preliminary report, using measurements based upon peak-to-peak analysis of fluorescence intensity in single perfused microvessels, demonstrates that the peak intensity of fluorescently labeled GCX components is 200–250 nm from the EC surface (47). By contrast, whole-width analysis of fluorescently labeled GCX provides a value of ~1.5 μm for the GCX surface layer depth (47). Cryopreservation may also fail to preserve a more compact ordered structure despite better retention of total material. A general problem observed under some conditions of fixation is increased secretion and/or leakage of cellular components to the cell surface that cannot be distinguished from the surface material.

Although there is growing consensus, based primarily on newer fixation and vessel lumen measures, that components of the GCX can extend much farther into the lumen than indicated by all early EM and optical methods, there are conflicting assessments of the value of the information that can be drawn from estimates of thickness alone. On one hand, there appears to be a relation between the thickness of the GCX and the decreased susceptibility of regions of the arterial wall to injury and atherosclerosis (48). As developed in more detail in a later section, there is also evidence from clinical studies that changes in the thickness of the GCX are an early indicator of critical changes in EC function in disease. An extension of this idea is to use an indicator dilution approach to estimate changes in the volume of the GCX in disease states (42), but in its present form, the approach has significant limitations as described by Michel & Curry (49). On the other hand, there is growing awareness of the limitations of measurements of GCX thickness to study the cellular and molecular mechanisms regulating mechanotransduction and EC barrier stability by the GCX. For

example, none of the fixation methods used to obtain the images in Figure 3 provides a way to link the observed ultrastructure to the chemical composition described above. Further, selective removal of known components of the GCX does not change measured thickness (26). These observations point to the need to understand at least some of the function of the GCX in terms of the spatial and temporal distribution of components on the EC surface.

Because the molecular weights of GAGs and core proteins would suggest lengths of the order of 100 nm, it follows that there are likely levels of structural organization within any GCX layer that extend many GAG lengths from the EC surface. It has been suggested that there is a soft (porous) outer layer that shows up in confocal immunofluorescence imaging that is not detected by purely physical techniques; only a stiffer less porous inner layer is observable by physical methods (12). Furthermore, in frog mesenteric capillaries (50) and in mammalian microvessels (51), 3D reconstruction of the GCX structure has been used to describe a quasi-ordered layer extending up to 200 nm from the EC surface. Curry & Adamson (9) reviewed these topics and suggested three principles of GCX organization as outlined below.

RELATION BETWEEN BIOCHEMICAL COMPOSITION AND ULTRASTRUCTURE: MECHANISMS FOR SIGNAL TRANSDUCTION FROM THE OUTSIDE IN

As suggested above, the first organizational principle that relates structure to function is that different components of the GCX modulate different levels of penetration of circulating macromolecules into the GCX. This is important because agents that modify EC function are often carried to the membrane surface bound to plasma proteins or other circulating complexes (e.g., RBCs, albumin, and HDLs in the case of S1P). Important insight into this aspect of layered structure of the GCX comes from investigations in which its function is evaluated before and after exposure to enzymes chosen to degrade specific components. Treatment with hyaluronidase in cremaster muscle vessels caused increased penetration of dextrans D70 and D145 (approximately 70 and 145 kDa, respectively), but there was no change in the exclusion of RBCs and anionic proteins. This barrier was restored by infusion of HA together with CS. By contrast, in the same vessels, treatment with heparinase was shown to cause a significant increase in the penetration of RBCs and white blood cells (52). Furthermore, Gao & Lipowsky (53) used heparinase, chondroitinase, and hyaluronidase in rat mesentery microvessels and found that a combination of all three enzymes reduced GCX thickness to ~10% of control thickness. However, individual enzymes reduced the surface layer thickness to between 50 and 65% of untreated values. From measurement of the rate of tracer penetration after chondroitinase and hyaluronidase treatment, these investigators found evidence for a denser GCX near the EC surface.

In cultured ECs, a variety of techniques are becoming available to further extend analysis of structure and composition. These include fluorescence correlation spectroscopy to probe albumin dynamics inside lung endothelial GCX (40) and new ways to preserve the layer, such as rapid freezing and freeze substitution, as illustrated in Figure 3 (33). The new generation of super-resolution optical microscopes, with resolution down to 20 nm, may

help to resolve the issue of composition and ultrastructure at the molecular scale with dynamic studies of ECs exposed to defined hydrodynamic stress or substrate strain (54).

A second organizational principle is that the high-molecular-weight GAG HA provides part of the scaffold for the EC surface layer. Attached to EC membrane receptors such as CD44, long chains of HA are presumed to intertwine through the GCX and contribute to the layered structure at distances above the EC surface much greater than the maximum extent of glycoproteins and other membrane-attached molecules. It remains to be determined if strands such as those indicated by arrows in Figure 3*c* represent HA perpendicular to the surface, rather than intertwined within the structure. Quantitative predictions of steric exclusion, restricted diffusion, and water flows within fiber matrices (55–58) show that the exclusion of macromolecules close to the size of albumin can be accounted for in a fibrous meshwork with fibers having radii less than 1 nm and that occupy 2–5% of the matrix volume. Such models can be extended to take into account different shapes of macromolecules as well as the effect of charge (56, 59).

A third organizational principle of the GCX concerns its dynamic nature. There is evidence that the thickness of the GCX is a balance between the rate of synthesis of GCX components and the rate of degradation (60, 61). Synthesis can be modulated by the supply of precursors of matrix components; degradation is modulated by endogenous enzymes including heparinase, hyaluronidase, and metalloproteases. Synthesis and degradation are likely to modify the observed rates of tracer penetration. For example, it is not unreasonable to suggest that penetration of test tracers may be significantly retarded if tracers are preferentially removed near the outer layers after binding to components of the GCX. Further, the addition of new components to the matrix also modulates the organization of matrix components. For example, the binding of new HA, which forms part of the outer layer of the GCX (Figure 2), to its membrane-linked binding proteins (e.g., CD44) causes clustering of the bound complex into endothelial caveolae and activation of S1P1 (62). Signaling via S1P1 stabilizes the cortical actin network in the EC periphery. These observations suggest that the function of the GCX may depend as much on the organization of anchoring points to the cell cytoskeleton and the modulation of associated signaling pathways as on the organization within the matrix itself.

The process may be further modified by synthesis of material to replace lost components of the matrix. There may also be dynamic rearrangement of components in response to flow. In a recent study, Zeng and colleagues (63) showed that when ECs in culture were exposed to fluid shear stress (FSS) for 30 min, HS, which covered the cell uniformly under static conditions, moved to the downstream cell boundaries (Figure 4), whereas CS did not move at all. In addition, syndecan-1 and caveolin-1 did not move, but lipid rafts were mobile and responded to shear. The authors concluded that glypican-1 bound to lipid rafts (not caveolae) carried HS, and not CS (recall Figure 2), downstream in response to shear. More recent work by the same group showed that after shear exposure for 24 h, the original uniform distribution of HS is restored as actin stress fibers develop that anchor membrane microdomains rich in newly synthesized HS (29). In the next section, we focus on the role of the glycocalyx as a modulator of mechanotransduction.

EVIDENCE FOR MECHANOTRANSDUCTION BY SURFACE PROTEOGLYCANS AND GLYCOPROTEINS

The primary evidence that supports a central role for the GCX in mechanotransduction comes from experiments involving use of enzymes to selectively degrade specific components of the GCX, followed by a reassessment of function. Florian et al. (64) used the enzyme heparinase III to selectively degrade the HS component of BAEC GAGs in vitro and observed that normal production of nitric oxide (NO) induced over 3 h by steady or oscillatory shear could be completely inhibited (Figure 5). In an earlier study, the enzyme neuraminidase was used to remove SA residues from saline-perfused rabbit mesenteric arteries, and it was observed that flow-dependent vasodilation was abolished by a 30-min enzymatic pretreatment (65). Because flow-dependent vasodilation is mediated by NO release in many arteries, this study suggests that SA also contributes to shear-induced production of NO. Similarly, Hecker et al. (66) showed that when intact segments of rabbit femoral arteries were pretreated with neuraminidase, shear-induced NO production was inhibited. In another study, the enzyme hyaluronidase was used in isolated canine femoral arteries to degrade HA from the GCX layer, and a significant inhibition of shear-induced NO production was demonstrated (67). Additional studies of flow-mediated vasodilation in mice using various manipulations of the GCX also support a role for the GCX in sensing and transducing FSS (68).

Rubio & Ceballos (69), using guinea pig hearts, showed a direct relationship between changes in GCX structure and the responses of coronary arteries to changes in coronary flow. Another in vitro study using BAECs examined all of the basic GCX degrading enzymes—heparinase, neuraminidase, hyaluronidase, and chondroitinase—and showed that NO induced by a steady shear stress was substantially blocked by heparinase, neuraminidase, and hyaluronidase, but not chondroitinase (70).

A related response of ECs to shear is their morphological and cytoskeletal remodeling. The early stages of these processes are observed within hours after exposure of cultured EC to shear, and the culmination is observed after 24–48 h of exposure when cells elongate and align in the direction of flow (71). This distinct morphological response has been used as an indicator of shear stress magnitude and direction in vivo (72) and is considered to be one of the hallmarks of EC response to FSS. Recent work has demonstrated that this quintessential response is mediated by the GCX.

Thi et al. (73) examined the redistribution of F-actin, vinculin, and several other proteins in response to 5 h of FSS in different bathing media. Media without protein or protein-containing media pretreated with heparinase were associated with a disruption of the GCX. In normal media, there was a severe disruption of the dense peripheral actin band, a formation of stress fibers, and a migration of vinculin to cell borders after exposure to FSS. This early remodeling was completely abolished when the integrity of the GCX was compromised. The early remodeling (at 5 h) described in Thi et al. (73) was further examined by Moon et al. (74), who showed that the distinct tendency for BAECs to align with the applied shear direction (even at 5 h) was abolished by pretreatment of the monolayer with heparinase. This remodeling process culminates in cell elongation and

strong alignment in the direction of shear after 24–48 h, but Dewey's group (75) showed that disruption of the GCX with heparinase completely blocks this characteristic elongation and alignment in the direction of shear after 24 h.

LIMITATIONS OF ENZYME DEGRADATION STUDIES

Although the use of enzymes to modify the GCX strongly indicates its importance in the response of ECs to shear stress, some of the limitations of these enzymes should be noted. One is that they modify not only the EC surface PGs but also PGs on the basal surface, which act as coreceptors with integrins for extracellular matrix (ECM) proteins. Only when the EC barrier is sufficiently tight will it restrict passage of proteins such as heparinases and chrondroitinases (70–80-kDa molecular weight). Unfortunately, the barrier properties of many cultured EC monolayers are compromised, and some leakage of larger molecules is known to occur, giving them access to basal surface PGs (56, 76). Another concern is that heparinases and chondroitinase have a strong positive charge at normal pH (isoelectric points close to 9), whereas hyaluronidase is strongly negatively charged (isoelectic point of 4.5). Because cationic macromolecules penetrate the GCX much more than anionic macromolecules do, the effect of charge on access of these enzymes to GCX components depends on local pH. Furthermore, cationic proteins compete for negative charge sites and may modify the GCX organization independent of their enzyme action (64, 77). It follows that enzyme degradation studies may bias estimates of the relative contribution of different GCX layers to barrier and mechanical functions. An evaluation of this important topic is warranted.

MOLECULAR AND CELLULAR MECHANISMS LINKING THE GLYCOCALYX TO NITRIC OXIDE PRODUCTION AND CELLULAR REMODELING

There are several possible mechanisms relating the GCX to NO production and EC remodeling. The simplest is based on the idea that GAGs are the shear sensors that transmit force to the cell by way of the core proteins. The hypothesis is that deflections of the fibers due to exposure to shear stress cause molecular displacement of signaling proteins in the endothelial cytoskeleton. Weinbaum and colleagues (11) modeled the deflection of clusters of deformable fibers arranged on the cell surface and extending up to 400 nm and found that these would cause molecular displacements of the order of 10 nm within the actin cytoskeleton of the ECs. Shorter (150-nm) fibers produced much smaller displacements and may not generate the displacements required for outside-in signaling. A prediction from the model is that fluid flow within the EC surface layer due to the applied FSS is restricted to the outer 10% of the surface layer. Structures below this surface region are not exposed to fluid shear forces (11, 78). Thus, in a matrix of 400-nm thickness, not all components of an inner layer (150-nm fiber clusters as well as other possible FSS sensors, such as ion channels and surface receptors or caveolae) are exposed directly to FSS. They are likely to respond to applied fluid shear only in the absence of the GCX. In the presence of an intact GCX, the applied FSS is transmitted to the cell as a solid mechanical force via the core proteins that interface with the cell membrane or cytoskeleton. This is somewhat analogous to the force of the wind blowing through the leaves of a tree being transmitted to the ground through the tree trunk.

A recent study (79) tested the hypothesis that the transmembrane syndecan-1 core protein that is linked to the cytoskeleton mediates EC remodeling in response to shear stress, whereas the membrane-bound glypican-1 core protein that is enriched in caveolae where signaling molecules such as endothelial nitric oxide synthase (eNOS) reside mediates eNOS activation and NO production (recall Figure 2). The authors showed that enzymatic removal of HS that resides on both syndecan-1 and glypican-1 blocked both shear-induced eNOS activation (phosphorylation at Ser1177) and EC remodeling. By contrast, gene knockdown of glypican-1 blocked only eNOS activation, not remodeling, and knockdown of syndecan-1 blocked only remodeling, not eNOS activation. This study demonstrates how the GCX can convert a single mechanical signal (shear stress) into diverse cellular responses through distinct core proteins.

Another possible mechanism follows from the observation that HS plays a role in the availability of arginine and its transporters close to the EC surface. HS displays high affinities for polycationic molecules, such as poly(L-arginine)s, and the binding sites for these ligands involve arginine residues (15, 80–82). Thus HSPGs may serve as a means of concentrating arginine close to the plasma membrane. For example, it was shown that HSPGs adsorbed to a surface undergo a conformational change when exposed to flow: Their core proteins unfold from a random coil to an extended filament, and their HS chains elongate by 35% (81). This finding was used to illustrate how sodium ions bound to HS could be delivered by the stretched GAGs to their transporter channels. An analogous hypothesis can be made for the case of L-arginine, but there is no direct evidence relating FSS and NO response to this mechanism. More generally, HSPGs play a cooperative role in signaling pathways activated by a wide range of ligands including the members of the fibroblast growth factor (FGF) family and their receptor tyrosine kinases, transforming growth factors (TGFs), bone morphogenetic proteins (BMPs), Wnt proteins, chemokines, and interleukins, as well as enzymes and enzyme inhibitors, lipases and apolipoproteins, and ECM and plasma proteins (83). It remains to be determined whether modification of HS on the endothelial surface also modifies signaling pathways in a manner specific to a particular ligand.

STRUCTURES THAT SENSE STRESS AT CELL–CELL JUNCTIONS

Shear stress of blood flow and the radial and circumferential tension due to the gradient in transmural pressure both can produce tension and strain in the plasma membrane of the endothelium that effectively signal a myriad of responses at the vascular wall (84). Vascular endothelial cadherin (VE-cadherin) constitutes one of the main adherens junction proteins providing a barrier between the vascular and tissue compartments. The cytoplasmic domain of VE-cadherin connects to the cytoskeleton through β-catenin and forms robust junctions through homophilic interactions with adjacent VE-cadherin receptors and the localization of other junction proteins. VE-cadherin functions as a mechanosensing unit in a complex with PECAM-1 and vascular endothelial growth factor receptor 2 (VEGFR2), the former of which is an Ig family transmembrane protein that also localizes to intercellular junctions and forms connections with adjacent ECs. The PECAM-1 cytoplasmic tail contains phosphotyrosines that interact with ERK (extracellular signal–regulated kinase), which serves to transactivate VEGFR2 in the production of NO. PECAM-1’s capacity to signal in

direct response to mechanical activation was demonstrated in two elegant studies, one that employed microbead attachment and torque application (85) and a second that used cyclic stretching of cells (86). Collins et al. (87) recently demonstrated that localized tensional forces on PECAM-1 result, surprisingly, in global signaling responses. Specifically, force-dependent activation of phosphatidylinositol 3-kinase (PI3K) downstream of PECAM-1 promotes cell-wide activation of integrins and the small GTPase RhoA. These signaling events facilitate changes in cytoskeletal architecture, including growth of focal adhesions and adaptive cytoskeletal stiffening. Several lines of evidence suggest that VE-cadherin functions mainly as an adapter in this system by mediating the physical association of PECAM-1 and VEGFR2. Part of the evidence has been derived from studying PECAM-1 knockout mice that are defective in NO-dependent vasodilation as a function of increased FSS. In addition, there are several lines of evidence indicating that PECAM-1 serves as a mechanosensor that contributes to atherogenesis. It is worth noting that there is uncertainty as to the mechanism by which the VEGFR2 functions as a mechanosensor. One view of the GCX described by Weinbaum and colleagues (11) suggests that fluid shear stress would not be transmitted directly to embedded transmembrane proteins on the endothelial surface, such as the VEGFR2, because the fluid shear near the cell surface is relatively low as compared with that at the outer layers of the GCX. In this scenario, the VEGFR2 would function as a mechanosensor only when the GCX was absent or damaged. Another interpretation is that components of the GCX interact directly with PECAM-1 and/or VEGFR2 to impart the shear force of fluid flow to these structures (88). This is clearly an area that deserves additional investigation. Furthermore, for key components of the GCX including the core proteins of the surface PGs, there is little information on molecular mechanisms that modify subcellular structures such as the VE-cadherin complex described above. Further studies are warranted to evaluate the change that occurs in this complex as specific components of the GCX are depleted by enzymes as described below.

INFLAMMATORY RESPONSES REGULATED BY FLUID SHEAR STRESS AND THE GLYCOCALYX

There is a wealth of histological evidence that inflammation manifests as a focal disease process, as atherosclerotic lesions in the aorta and arteries occur within specific regions. Nascent plaque development in arteries occurs preferentially within characteristic geometries, such as curvatures and bifurcations that exhibit disturbed flow characteristics (89, 90). A hallmark of atherogenesis is the upregulation of EC adhesion molecules (CAMs) and concomitant recruitment of monocytes, which rapidly emigrate across inflamed ECs and over time differentiate into foam cells within the vessel intima. There is also evidence that the GCX plays a role in the focal nature of the inflammatory response, as it may participate in conversion of stress at the vascular interface or transmission of strain across the membrane to the cytoskeleton and nucleus. It is currently unknown precisely which membrane molecules and microdomains, including ion channels, receptors, G-proteins, adhesion molecules, the cytoskeleton, and caveolae, cooperate with the GCX in this signaling process.

Blood flow is laminar within the straight portions of blood vessels but may become disturbed at sites of curvature and at branch points, resulting in flow stagnation, recirculation, and the formation of downstream eddies. Shear stress imparted by the viscous flow of blood plays a significant role in the homeostasis of vascular structure and function, in part through the action of the mechanically responsive endothelium. The presence of low (i.e., ~1-dyn/cm^2) FSS, high gradients of stress, and flow disturbances all correlate with atherogenesis, whereas relatively high laminar shear is required to maintain vessel homeostasis (91). Thus, the magnitude of FSS and the level of cytokine stimulation tightly regulate where and when in arteries monocyte recruitment occurs. For instance, arterial regions of low FSS and large spatial gradients exhibit amplified upregulation of VCAM-1 and E-selectin, which in turn increase the efficiency of monocyte capture even at very low concentrations of cytokine stimulation [e.g. tumor necrosis factor alpha (TNF-α); 0.1 ng/mL] (92). Elevated levels (i.e., ~15 dyn/cm^2) of FSS as observed in arteries of healthy human subjects are atheroprotective. This is, in part, attributed to the mechanical influence of FSS acting on endothelium that results in attenuation of VCAM-1 expression, despite the fact that ICAM-1 expression is upregulated at high FSS.

The acute response to inflammatory signaling at the vascular interface is upregulation of adhesion receptors and elaboration of chemokines that are expressed on the endothelial surface (93). This initiates capture of leukocytes from flowing blood, which requires a precise balance of cell adhesive forces formed by noncovalent molecular bonds that overcome the hemodynamic FSS. The relative expression level of adhesion receptors is dependent not only on the magnitude of shear stress but also on temporal and spatial variations of FSS (8). The greatest change in TNF-α-stimulated VCAM-1 and E-selectin expression on inflamed human aortic endothelial cells (HAECs) is observed within the low range in shear, from 1 to 4 dyn/cm^2, that corresponds with levels observed within atherosusceptible regions (94). Higher levels on the order of 10 dyn/cm^2 actually suppress upregulation of these receptors but promote elevated expression of ICAM-1, which is associated with immunosurveillance of neutrophils and monocytes. Expression of E-selectin and VCAM-1 is invariant at shear greater than 10 dyn/cm^2, a rate that correlates with atheroprotective endothelial responses within straight unperturbed regions of arterial flow (i.e., 10–16 dyn/cm^2) (8).

Although the precise mechanisms by which shear superposes with cytokine to regulate inflammatory gene expression have yet to be determined, it is clear that they act through distinct and convergent transduction pathways to modulate the activity of transcription factors associated with inflammation, including nuclear factor-kappaB (NFκB), activator protein-1 (AP-1), GATA, specificity protein-1 (SP-1), and IFN regulatory factor-1 (IRF-1) (95). Activation of these factors and their binding to distinct promoter regions can account for the induction or suppression of inflammatory genes as described below. NFκB (p65/p50 heterodimer) is known to bind a cis-acting FSS-responsive element and mediate the expression of many cytokine-induced genes active during vascular inflammation and atherogenesis.

The relationship between FSS and transcriptional control of CAM expression was examined by measuring the pattern of phospho-p65 translocation in an in vitro flow channel in which

FSS increased linearly from 0 up to 12 dyn/cm^2. NFκB activity most closely matched upregulation of ICAM-1, as both increased along the shear stress gradient (92). This pattern of regulation is consistent with the fact that the *ICAM-1* gene has functional binding sites for NFκB. Notably, these studies found that phospho-p65 levels were not elevated at low (~2 dyn/cm^2) FSS or under static control conditions, even though this was the regime over which VCAM-1 and E-selectin upregulation was greatest. This was surprising because both VCAM-1 and E-selectin promoters contain binding sites for NFκB. One explanation is that VCAM-1 and E-selectin are more sensitive to downregulation of c-Jun N-terminal kinase (JNK) and p38 mitogen-activated protein kinases (MAPKs), which are activated by distinct pathways that appear to involve upregulation of interferon regulatory factor 1 (IRF-1) (95). Such a mechanism could be modulated by different components of the GCX that respond and transduce signals differentially based upon the magnitude of FSS. In this manner, although all three gene products are influenced by NFκB translocation, ICAM-1 transcription is modulated differently through the GCX, which effectively transduces signal as a function of the magnitude of FSS.

Structural changes in the GCX may represent the initial response that alters the atherogenecity of ECs. One prominent mechanism that has been proposed involves an increase in the affinity of lipoproteins to bind to the EC surface following cleavage of HS and HA from the GCX in atheroprone regions of disturbed flow in the carotid bifurcation (46). A recent paper by Koo et al. (31) indicated that the GCX can be differentially regulated by distinct FSS waveforms. HS expression on the proteoglycan syndecan-1 was shown to increase in a uniform pattern on the apical surface of ECs exposed to the atheroprotective waveform. By contrast, its expression was irregularly present on ECs exposed to a waveform simulating an atheroprone shear regime. Moreover, suppression of syndecan-1 diminished the atheroprotective flow-induced cell surface expression of HS. Higher FSS increases the rate of GCX biosynthesis, as demonstrated for porcine aortic endothelium (96). In this manner, GCX density and composition may vary as a function of position in arteries and more efficiently downregulate transcriptional activity in high-FSS regions. In addition to the GCX, there are several other candidates that may function as shear-sensitive transducers at the EC surface in distinct regions of arteries. Both membrane glycoproteins and integrins have been reported to sense mechanical stress and to exhibit signaling capacity as a function of spatial distribution; however, the precise mechanisms are not completely defined.

BLOOD CELL–ENDOTHELIAL CROSS TALK CATALYZED BY FLUID SHEAR STRESS

Leukocyte recruitment to inflamed ECs requires recognition of receptors and counterreceptors expressed on adjacent cell membranes. The various moieties that constitute the GCX may exert both steric and electrostatic influences on the balance of free energy required to overcome the repulsive shear force of blood flow. E- and P-selectins, which are expressed on ECs and extend about 30 nm above the endothelial surface, function to initially capture leukocytes from the free stream. These glycoproteins are presumably buried within the GCX that extends several micrometers from the EC surface in regions where the GCX is

intact. Leukocytes possess microvilli with lengths of 300 to 700 nm. Upon cell contact and rolling on inflamed ECs, microvilli may provide a means of penetration through the GCX (97). Thus, interaction between receptors on ECs and their selectin ligands on rolling leukocytes would involve the penetration of microvilli through the GCX to form point contacts. Such a mechanism would depend upon the relative porosity of GCX versus the stiffness of the leukocyte microvilli. Conversion to stable adhesion and leukocyte activation that lead to transendothelial migration also require intimate contacts such that leukocytes form sufficient bonds between integrins and Ig superfamily members, including ICAM-1 and VCAM-1, on ECs. In addition, ligation of chemokine receptors with their cognate ligands that have affinity domains for HS on the GCX is also a necessary step for signaling of additional integrin activation and actin-driven leukocyte motility. Thus, access of integrins, selectins, and chemotactic receptors to their respective ligands on an adjacent cell is essential for efficient adhesion and activation during inflammation and immunosurveillance. In a recent review on the subject, Gao & Lipowsky (53) summarized it aptly, stating there was “an underlying connection between integrity of the GCX and vascular homeostasis.” A predominant mechanism influencing the recruitment of leukocytes is binding and presentation of plasma-derived chemokines, pro- and anticoagulants/oxidants, and growth factors. Regulation of the thickness and composition of GCX by local gradients of FSS and the presence of enzymes that can degrade it may directly influence the net negative charge and the local concentration of agonists and receptors that activate and bind to flowing leukocytes. It is well demonstrated that shedding of the GCX is precipitated by cell activation via cytokines and chemoattractants, and this can occur throughout the microvasculature, including capillaries, venules, and arterioles (53). In pathological situations such as sepsis, hyperglycemia, and atherosclerosis, the GCX may be exposed to oxidized low-density lipoprotein (oxLDL), TNF-α, atrial natriuretic peptide, and ischemia, which have all been shown to elicit GCX shedding (98). Thus, differential regulation of CAM transcription and expression results in changes that exert both pro- and anti-inflammatory actions on leukocyte recruitment (99–102). The focal nature of atherosclerosis, in which monocyte recruitment is observed at bifurcations and curved arteries that harbor steep FSS gradients and disturbances, may be related to changes in the local dimensions of the GCX. A more detailed study of how CAM expression and monocyte recruitment, as well as local variation in GCX, map onto inflamed endothelium exposed to shear is of keen interest.

S1P AND THE ENDOTHELIUM

There is strong cross talk between RBCs, platelets, and endothelium owing to the actions of S1P. As described above, exogenous S1P plays a key role in stabilizing the GCX under EC culture (63). These observations are part of a growing understanding of the role of endogenous S1P in the vascular system: It acts to stabilize not only the surface GCX but also the whole EC barrier, thereby modifying the response to shear stress, inflammatory agents, and interactions with immune cells (103). S1P is found in plasma at a concentration of ~0.2 to 0.5 μM and is synthesized from sphingosine via two sphingosine kinases (Sphk1 and Sphk2) (104, 105). Although many cells synthesize and release S1P, including ECs in response to shear, the predominant source of S1P under normal circulatory conditions is the

RBCs that release S1P continuously and without stimulation (104, 106, 107). After synthesis, S1P is preferentially stored in RBCs and released continuously via a novel adenosine 5′-triphosphate (ATP)-dependent transporter (104, 107). The importance of RBCs as a primary source of circulating S1P is demonstrated by directed knockout of RBC Sphk1 and Sphk2 resulting in increased basal permeability in mouse organs, including lung and skin, and in increased susceptibility to inflammatory agents (108). This condition is reversed by reinfusion of wild-type RBCs. Plasma HDL (apolipoprotein M) and serum albumin enhance release and subsequent transport of S1P bound to arginine-rich sites on the plasma proteins (109). Platelets are also an abundant source of S1P, but they do not appear to contribute significantly to normal circulating levels. S1P release from platelets depends on stimulation by inflammatory mediators and local injury (110, 111). S1P acts to stabilize the EC permeability barrier by binding to S1P1 and signaling via the small GTPase Rac1 (Figure 6, *bottom*).

Downstream cellular targets include the actin-binding protein cortactin to stabilize the cortical actin network and the junctional complex organizing the adherens junction protein VE-cadherin (103, 112). The Rho family GTPase Rac1 is activated by S1P in ECs, and permeability is directly dependent upon exogenous S1P added to the perfusion buffer (113). A threshold level of S1P concentration (100–300 nM) is required for stable EC barrier function (114). A recent study (29) also shows that the GCX is degraded by the release of MMPs when S1P levels drop below this critical range and S1P1 is vacated, as illustrated in Figure 6 (*top*). Loss of GCX in a low-S1P environment is also expected to contribute to the loss of EC barrier function (76). The relative contributions of junction integrity (Figure 6, *bottom*) and GCX integrity (Figure 6, *top*) to the stability of the EC transport barrier have not been assessed, and this remains an important question for future studies. Within the scope of this review, it is important to emphasize that observations establishing a role of S1P in maintaining the EC GCX and a low permeability state indicate the need for reevaluation of earlier observations for which the amount of S1P (from either endogenous or exogenous sources) in culture media, artificial perfusates, and circulating blood was not measured or reported. The amount of fetal calf serum (FCS) used to supplement culture medium varies from 5 to 20%, and FCS-containing culture medium is often replaced by minimum essential medium (MEM) containing 1% (10 mg/mL) albumin. RBCs are almost never added to medium. Therefore, there is great variation in the supply of S1P. In culture media containing 5% FCS, S1P concentrations are close to 100 nM, and they are close to 50–70 nM in solutions containing 1% bovine serum albumin (29). These S1P concentrations fall near, or below, levels at which the stability of endothelial surface glycoproteins is disrupted, and they fall below normal plasma S1P levels that ensure stable vascular barrier permeability. Higher concentrations of S1P are expected in bathing fluids when FCS concentration is greater than 5% and when albumin concentrations exceed 1%, but information about the stability of S1P under different culture conditions and in artificial perfusate is lacking. These observations highlight the importance of understanding (*a*) how the initial conditions of an EC barrier determine its response to changes in perfusion conditions and (*b*) the relative contribution of flow-sensing mechanisms directly linked to the stability of the GCX and mechanisms reflecting the stability of the whole EC layer. For example, the amount of fetal bovine serum (FBS) in media not only contributes to S1P levels but also can modulate cell

turnover, cell motility, and tight junction breakdown. Lower levels of FBS reduce cell turnover and junction breakdown (115). Thus, the contribution of S1P from endogenous sources to changes in endothelial barrier responses to a wide range of experimental conditions is an area for further investigation.

S1P AND ENDOTHELIAL RESPONSE TO SHEAR STRESS IN THE MICROCIRCULATION

In an intact microcirculation conditioned by constant blood perfusion, S1P from RBCs actively maintains a low permeability state (116). In individually perfused microvessels, rapid switching between artificial perfusates to enable removal of S1P followed by S1P replacement results in correspondingly rapid increases and restoration of the vascular permeability barrier. This demonstrates that S1P regulates normal baseline permeability and acts in a dynamic fashion to maintain a basal vascular permeability tone (9, 113). Adamson and colleagues (114) have recently demonstrated that a constant supply of S1P is necessary to ensure that vascular permeability to water and macromolecules is stable and independent of shear over a wide range of FSS. These results begin to explain the sustained stability of microvessels to water and macromolecules under a wide range of perfusate flows when RBCs are present (e.g., the modified Landis technique of measuring single-vessel permeability), as reported by a number of laboratories (9, 117, 118). However, this does not rule out subtle shear-dependent regulation of barrier permeability, including transient changes in water permeability in intact vessels and regulation of the permeability of the barrier to low-molecular-weight molecules (3, 119, 120).

In microvessels, although the stable permeability state is independent of shear-stress magnitude, it is significantly disrupted by disturbed flow (114). In contrast to stable permeability barriers found even after hours of microperfusion in the direction of normal blood flow, microvessels of rat mesentery exposed to 90 min of flow in the direction opposite to normal blood flow (retrograde perfusion) undergo an increase in vascular permeability. These findings for microvessels are consistent with recent observations in cell culture models that retrograde flow imposed after flow conditioning results in reorientation of the angle of intercellular junctions to the direction of flow (61).

All the above observations of the sustained stability of the EC barrier to water and macromolecules under a range of experimental conditions when S1P is available were made for microvessels. At this stage in the development of our understanding of S1P-dependent modulation of permeability and mechanosensing, it is useful to distinguish between microvessels, on one hand, and arteries and cultured monolayers derived from the arteries, on the other. Even taking into consideration the concerns expressed above about the initial state of the EC barriers and the modulation of response by the composition of culture media, there is compelling evidence for shear-dependent regulation of water and macromolecule permeability and for a role for the GCX in shear-dependent NO production, also reviewed above (121). Similar considerations apply in intact vessels ranging from isolated coronary venules (122) to aortic segments (123, 124). There is a clear need to understand these differences and the role of S1P-dependent pathways in the well-described observation that disturbed flow in larger vessels increases local permeability to macromolecules and

susceptibility to inflammatory stimuli (125). Other mechanisms to be investigated in arterial segments include the shear-dependent regulation of the permeability of low-molecular-weight (<500-kDa) nutrient molecules, the shear-dependent regulation of endothelial adhesion receptor expression (126), the role of changes in GCX structure on the selective barrier in the artery wall (9), and the mechanisms by which S1P-dependent Rac1 activation modulates both shear-dependent reactive oxygen species (ROS) generation and vascular permeability (127).

S1P AND FLOW-MEDIATED RESPONSES INVOLVING OTHER VASCULAR CELLS

There is evidence that loss of the GCX increases immune cell access to the EC surface. Based on the role of S1P in stabilizing the GCX, it is expected that the absence of S1P would contribute to immune cell attachment to the vascular surface. In addition, one of the best-studied roles of S1P in vascular function is regulation of the egress of immune cells from lymphoid tissue and their circulation back into lymph and blood (128–130). S1P concentrations in plasma and lymph, in the submicromolar range, are higher than those in interstitial fluid and are regulated by multiple mechanisms (128). Compared with detailed knowledge of the multistep mechanisms of lymphocyte attachment, rolling, tight binding, and transmigration at the endothelial surface, S1P-dependent immune cells distribution after crossing the endothelial barrier is far less well understood.

Recent observations provide important new insight into the role of S1P and S1P1 to transduce flow-mediated signaling in ECs both in vitro and in vivo. Jung et al. (131) described a gradient of S1P1 from the mature regions of the vascular network to the growing vascular front. In the absence of endothelial S1P1, adherens junctions are destabilized and barrier function is reduced. This result is not surprising given the tonic role of S1P in stabilizing the endothelial barrier, as described above. In addition, there is abnormal vascular hypersprouting when S1P1 is absent. In intact vasculature, the authors found that S1P1 is most prominent in the EC membrane in regions of the aorta with laminar shear stress.

PATHOPHYSIOLOGICAL FUNCTIONS OF THE GLYCOCALYX

The association of altered GCX characteristics with atherosclerosis-prone locations in arteries was recognized in the early 1980s. Lewis et al. (132) observed the coronary arteries of White Carneau pigeons and noted that the GCX, as assessed by ruthenium red staining, was thinnest in areas with high disease predilection and that upon cholesterol challenge, the GCX thickness was reduced in all arterial zones. This idea of association between GCX abundance and arterial disease was revisited by Van den Berg et al. (48), who showed that GCX thickness in the disease-prone sinus region of the mouse internal carotid artery was significantly less than that in the nearby common carotid artery that was spared of disease. These observations are consistent with studies demonstrating that GCX components are synthesized at a higher rate when arteries are exposed to high wall shear stress versus low wall shear stress and that the GCX is shed from the EC surface after exposure to ox-LDL or other inflammatory agents (60). These mechanisms can explain the observed lower GCX thickness in the low-shear-stress carotid sinus relative to that in the higher-shear-stress

common carotid. Van den Berg et al. (46) observed enhanced intimal accumulation of LDL in the internal carotid branch of mice where the EGL was thinner than in adjacent regions of the common carotid. The authors hypothesized that impaired GCX barrier properties were responsible for the enhanced LDL accumulation. Nagy et al. (68) found that inhibition of HA synthesis in a mouse model interfered with the protective function of the GCX, thereby facilitating leukocyte adhesion, subsequent inflammation, and progression of atherosclerosis.

In vitro models of hyperglycemia associated with diabetes are characterized by loss of HS and of FSS mechanotransduction, most notably the loss of elongation of ECs in the direction of shear (133) and the phosphorylation of eNOS in response to FSS (134). The observations that with diabetes, atherosclerosis is distributed more uniformly in arteries rather than limited to the typical atherogenic regions (regions of low shear or disturbed flow) near bifurcations and curvatures (135) and that vasodilation is altered (136) suggest that there is something fundamentally different in the mechanosensing apparatus of ECs during disease and may be explained in part by alterations in GCX.

Patients with renal failure have endothelial dysfunction and increased risk for cardiovascular morbidity and mortality. Using sidestream dark-field imaging, Viahu et al. (137) determined that dialysis patients had an impaired GCX barrier and shed HA and syndecan-1 into their blood. The role of dysfunction of the EC GCX in the glomerulus that leads to albuminuria has been reviewed by Salmon et al. (138), which includes a discussion of systemic increases in microvascular permeability. Alterations in sublingual microvascular permeability and GCX thickness in lacunar stroke patients with white matter lesions are associated with loss of GCX as well (43).

UNRESOLVED ISSUES AND FUTURE DIRECTIONS

The relationship between the ultrastructural and biochemical organization of the GCX remains to be determined directly. This will require the application of new high-resolution microscopy methods to samples with individually labeled components. The distribution of GCX core protein anchors among various compartments of the EC plasma membrane (caveolae and lipid rafts) and transmembrane linkages also remain to be determined. This knowledge will clarify how a mechanical signal like shear stress can be distributed into an array of cellular responses that exert differential effects, such as on expression and function of vascular adhesion molecules. The relative contributions of the GCX and the cytoskeleton to the control of EC permeability/hydraulic conductivity when the concentration of S1P is varied remain to be established. Low S1P levels in low-serum media in vitro may lead to a nonphysiological environment. Pharmaceutical or other biological approaches to the enhancement of GCX components need to be developed as tools to impede or reverse the development of vascular diseases related to atherosclerosis, diabetes, hypertension, and others.

Acknowledgments

We thank Drs. Tony Passerini, Roger Adamson, and Eno Ebong for generous editorial assistance. Funding has been provided by the NIH: AI47294 and HL082689 to S.I.S., HL 28607 and HL 44485 to F.E.C., and HL57093 and HL94889 to J.M.T.

Glossary

ECs	endothelial cells
GCX	glycocalyx
S1P	sphingosine-1 phosphate
GAG	glycosaminoglycan
HS	heparan sulfate
CS	chondroitin sulfate
HA	hyaluronic acid
GPI	glycosylphosphatidylinositol
BAECs	bovine aortic endothelial cells
RFPECs	rat fat pad endothelial cells

LITERATURE CITED

1. Nerem RM, Levesque MJ, Cornhill JF. Vascular endothelial morphology as an indicator of the pattern of blood flow. J Biomech Eng. 1981; 103:172–76. [PubMed: 7278195]
2. Kuchan MJ, Frangos JA. Role of calcium and calmodulin in flow-induced nitric oxide production in endothelial cells. Am J Physiol. 1994; 266:C628–36. [PubMed: 8166225]
3. Frangos JA, Eskin SG, McIntire LV, Ives CL. Flow effects on prostacyclin production by cultured human endothelial cells. Science. 1985; 227:1477–79. [PubMed: 3883488]
4. Mo M, Eskin SG, Schilling WP. Flow-induced changes in Ca^{2+} signaling of vascular endothelial cells: effect of shear stress and ATP. Am J Physiol. 1991; 260:H1698–707. [PubMed: 2035689]
5. Tarbell JM, Shi ZD, Dunn J, Jo HJ. Fluid mechanics, arterial disease and gene expression. Annu Rev Fluid Mech. 2014; 46:591–614. [PubMed: 25360054]
6. Chatzizisis YS, Coskun AU, Jonas M, Edelman ER, Feldman CL, Stone PH. Role of endothelial shear stress in the natural history of coronary atherosclerosis and vascular remodeling: molecular, cellular, and vascular behavior. J Am Coll Cardiol. 2007; 49:2379–93. [PubMed: 17599600]
7. Resnick N, Collins T, Atkinson W, Bonthron DT, Dewey CF Jr, Gimbrone MA Jr. Platelet-derived growth factor B chain promoter contains a cis-acting fluid shear-stress-responsive element. Proc Natl Acad Sci USA. 1993; 90:4591–95. [PubMed: 8506304]
8. Davies PF. Hemodynamic shear stress and the endothelium in cardiovascular pathophysiology. Nat Clin Pract Cardiovasc Med. 2009; 6:16–26. [PubMed: 19029993]
9. Curry FE, Adamson RH. Endothelial glycocalyx: permeability barrier and mechanosensor. Ann Biomed Eng. 2012; 40:828–39. [PubMed: 22009311]
10. Tarbell JM, Pahakis MY. Mechanotransduction and the glycocalyx. J Intern Med. 2006; 259:339–50. [PubMed: 16594902]
11. Weinbaum S, Tarbell JM, Damiano ER. The structure and function of the endothelial glycocalyx layer. Annu Rev Biomed Eng. 2007; 9:121–67. [PubMed: 17373886]
12. Pries AR, Secomb TW, Gaehtgens P. The endothelial surface layer. Pflugers Arch. 2000; 440:653–66. [PubMed: 11007304]

13. Seog J, Dean D, Rolauffs B, Wu T, Genzer J, et al. Nanomechanics of opposing glycosaminoglycan macromolecules. J Biomech. 2005; 38:1789–97. [PubMed: 16023465]
14. Oohira A, Wight TN, Bornstein P. Sulfated proteoglycans synthesized by vascular endothelial cells in culture. J Biol Chem. 1983; 258:2014–21. [PubMed: 6337150]
15. Jackson RL, Busch SJ, Cardin AD. Glycosaminoglycans: molecular properties, protein interactions, and role in physiological processes. Physiol Rev. 1991; 71:481–539. [PubMed: 2006221]
16. Rosenberg RD, Shworak NW, Liu J, Schwartz JJ, Zhang L. Heparan sulfate proteoglycans of the cardiovascular system: Specific structures emerge but how is synthesis regulated? J Clin Investig. 1997; 100:S67–75. [PubMed: 9413405]
17. Halden Y, Rek A, Atzenhofer W, Szilak L, Wabnig A, Kungl AJ. Interleukin-8 binds to syndecan-2 on human endothelial cells. Biochem J. 2004; 377:533–38. [PubMed: 14527339]
18. Kokenyesi R, Bernfield M. Core protein structure and sequence determine the site and presence of heparan sulfate and chondroitin sulfate on syndecan-1. J Biol Chem. 1994; 269:12304–9. [PubMed: 8163535]
19. Simons M, Horowitz A. Syndecan-4-mediated signalling. Cell Signal. 2001; 13:855–62. [PubMed: 11728825]
20. Yoneda A, Couchman JR. Regulation of cytoskeletal organization by syndecan transmembrane proteoglycans. Matrix Biol. 2003; 22:25–33. [PubMed: 12714039]
21. Fransson LA, Belting M, Cheng F, Jonsson M, Mani K, Sandgren S. Novel aspects of glypican glycobiology. Cell Mol Life Sci. 2004; 61:1016–24. [PubMed: 15112050]
22. Cheng F, Mani K, Van den Born J, Ding K, Belting M, Fransson LA. Nitric oxide-dependent processing of heparan sulfate in recycling S-nitrosylated glypican-1 takes place in caveolin-1-containing endosomes. J Biol Chem. 2002; 277:44431–39. [PubMed: 12226079]
23. Van Deurs B, Roepstorff K, Hommelgaard AM, Sandvig K. Caveolae: anchored, multifunctional platforms in the lipid ocean. Trends Cell Biol. 2003; 13:92–100. [PubMed: 12559760]
24. Laurent TC, Fraser JR. Hyaluronan. FASEB J. 1992; 6:2397–404. [PubMed: 1563592]
25. Henry CB, Duling BR. Permeation of the luminal capillary glycocalyx is determined by hyaluronan. Am J Physiol. 1999; 277:H508–14. [PubMed: 10444475]
26. Zeng Y, Ebong EE, Fu BM, Tarbell JM. The structural stability of the endothelial glycocalyx after enzymatic removal of glycosaminoglycans. PLoS ONE. 2012; 7:e43168. [PubMed: 22905223]
27. Adamson RH, Clough G. Plasma proteins modify the endothelial cell glycocalyx of frog mesenteric microvessels. J Physiol. 1992; 445:473–86. [PubMed: 1501143]
28. Curry FE, Adamson RH. Sphingosine-1-phosphate and the “albumin effect” on rat venular microvessels. FASEB J. 2013; 27(Suppl):896.2.
29. Zeng Y, Adamson RH, Curry FR, Tarbell JM. Sphingosine-1-phosphate protects endothelial glycocalyx by inhibiting syndecan-1 shedding. Am J Physiol Heart Circ Physiol. 2014; 306:H363–72. [PubMed: 24285115]
30. Giantsos-Adams KM, Koo AJ, Song S, Sakai J, Sankaran J, et al. Heparan sulfate regrowth profiles under laminar shear flow following enzymatic degradation. Cell Mol Bioeng. 2013; 6:160–74. [PubMed: 23805169]
31. Koo A, Dewey CF, García-Cardeña G. Hemodynamic shear stress characteristic of atherosclerosis-resistant regions promotes glycocalyx formation in cultured endothelial cells. Am J Physiol-Cell Physiol. 2013; 304:C137–46. [PubMed: 23114962]
32. Reitsma S, Slaaf DW, Vink H, Van Zandvoort MA, oude Egbrink MG. The endothelial glycocalyx: composition, functions, and visualization. Pflugers Arch. 2007; 454:345–59. [PubMed: 17256154]
33. Ebong EE, Macaluso FP, Spray DC, Tarbell JM. Imaging the endothelial glycocalyx in vitro by rapid freezing/freeze substitution transmission electron microscopy. Arterioscler Thromb Vasc Biol. 2011; 31:1908–15. [PubMed: 21474821]
34. Rostgaard J, Qvortrup K. Electron microscopic demonstrations of filamentous molecular sieve plugs in capillary fenestrae. Microvasc Res. 1997; 53:1–13. [PubMed: 9056471]

35. Vink H, Duling BR. Identification of distinct luminal domains for macromolecules, erythrocytes, and leukocytes within mammalian capillaries. Circ Res. 1996; 79:581–89. [PubMed: 8781491]
36. Smith ML, Long DS, Damiano ER, Ley K. Near-wall micro-PIV reveals a hydrodynamically relevant endothelial surface layer in venules in vivo. Biophys J. 2003; 85:637–45. [PubMed: 12829517]
37. Long DS, Smith ML, Pries AR, Ley K, Damiano ER. Microviscometry reveals reduced blood viscosity and altered shear rate and shear stress profiles in microvessels after hemodilution. Proc Natl Acad Sci USA. 2004; 101:10060–65. [PubMed: 15220478]
38. Damiano ER, Long DS, Smith ML. Estimation of viscosity profiles using velocimetry data from parallel flows of linearly viscous fluids: application to microvascular haemodynamics. J Fluid Mech. 2004; 512:1–19.
39. Barker AL, Konopatskaya O, Neal CR, Macpherson JV, Whatmore JL, et al. Observation and characterisation of the glycocalyx of viable human endothelial cells using confocal laser scanning microscopy. Phys Chem Chem Phys. 2004; 6:1006–11.
40. Stevens AP, Hlady V, Dull RO. Fluorescence correlation spectroscopy can probe albumin dynamics inside lung endothelial glycocalyx. Am J Physiol Lung Cell Mol Physiol. 2007; 293:L328–35. [PubMed: 17483194]
41. Yen WY, Cai B, Zeng M, Tarbell JM, Fu BM. Quantification of the endothelial surface glycocalyx on rat and mouse blood vessels. Microvasc Res. 2012; 83:337–46. [PubMed: 22349291]
42. Broekhuizen LN, Lemkes BA, Mooij HL, Meuwese MC, Verberne H, et al. Effect of sulodexide on endothelial glycocalyx and vascular permeability in patients with type 2 diabetes mellitus. Diabetologia. 2010; 53:2646–55. [PubMed: 20865240]
43. Martens RJ, Vink H, Van Oostenbrugge RJ, Staals J. Sublingual microvascular glycocalyx dimensions in lacunar stroke patients. Cerebrovasc Dis. 2013; 35:451–54. [PubMed: 23735841]
44. Megens RT, Reitsma S, Schiffers PH, Hilgers RH, De Mey JG, et al. Two-photon microscopy of vital murine elastic and muscular arteries: combined structural and functional imaging with subcellular resolution. J Vasc Res. 2007; 44:87–98. [PubMed: 17192719]
45. Reitsma S, Egbrink MG, Vink H, Van den Berg BM, Passos VL, et al. Endothelial glycocalyx structure in the intact carotid artery: a two-photon laser scanning microscopy study. J Vasc Res. 2011; 48:297–306. [PubMed: 21273784]
46. Van den Berg BM, Spaan JA, Vink H. Impaired glycocalyx barrier properties contribute to enhanced intimal low-density lipoprotein accumulation at the carotid artery bifurcation in mice. Pflugers Arch. 2009; 457:1199–206. [PubMed: 18839207]
47. Betteridge KB, Neal CR, Bates DO, Salmon AHJ. Endothelial glycocalyx-surface layer depth measurements in single perfused microvessels by confocal microscopy in vivo and subsequent electron microscopy. Microcirculation. 2013; 20:64.
48. Van den Berg BM, Spaan JA, Rolf TM, Vink H. Atherogenic region and diet diminish glycocalyx dimension and increase intima-to-media ratios at murine carotid artery bifurcation. Am J Physiol Heart Circ Physiol. 2006; 290:H915–20. [PubMed: 16155109]
49. Michel CC, Curry FR. Glycocalyx volume: a critical review of tracer dilution methods for its measurement. Microcirculation. 2009; 16:213–19. [PubMed: 19184776]
50. Squire JM, Chew M, Nneji G, Neal C, Barry J, Michel C. Quasi-periodic substructure in the microvessel endothelial glycocalyx: A possible explanation for molecular filtering? J Struct Biol. 2001; 136:239–55. [PubMed: 12051903]
51. Arkill KP, Neal CR, Mantell JM, Michel CC, Qvortrup K, et al. 3D reconstruction of the glycocalyx structure in mammalian capillaries using electron tomography. Microcirculation. 2012; 19:343–51. [PubMed: 22324320]
52. Desjardins C, Duling BR. Heparinase treatment suggests a role for the endothelial cell glycocalyx in regulation of capillary hematocrit. Am J Physiol. 1990; 258:H647–54. [PubMed: 2316679]
53. Gao L, Lipowsky HH. Composition of the endothelial glycocalyx and its relation to its thickness and diffusion of small solutes. Microvasc Res. 2010; 80:394–401. [PubMed: 20600162]
54. Sahl SJ, Moerner WE. Super-resolution fluorescence imaging with single molecules. Curr Opin Struct Biol. 2013; 23:778–87. [PubMed: 23932284]

55. Curry FE, Michel CC. A fiber matrix model of capillary permeability. Microvasc Res. 1980; 20:96–99. [PubMed: 7412590]
56. Michel CC, Curry FE. Microvascular permeability. Physiol Rev. 1999; 79:703–61. [PubMed: 10390517]
57. Ogston AG. The spaces in a uniform random suspension of fibres. Trans Faraday Soc. 1958; 54:1754–57.
58. Ogston AG, Michel CC. General descriptions of passive transport of neutral solute and solvent through membranes. Prog Biophys Mol Biol. 1978; 34:197–217. [PubMed: 375302]
59. Michel CC. Capillary permeability and how it may change. J Physiol. 1988; 404:1–29. [PubMed: 3075669]
60. Gouverneur M, Berg B, Nieuwdorp M, Stroes E, Vink H. Vasculoprotective properties of the endothelial glycocalyx: effects of fluid shear stress. J Intern Med. 2006; 259:393–400. [PubMed: 16594907]
61. Melchior B, Frangos JA. $G\alpha_{q/11}$-mediated intracellular calcium responses to retrograde flow in endothelial cells. Am J Physiol Cell Physiol. 2012; 303:C467–73. [PubMed: 22700794]
62. Singleton PA, Dudek SM, Ma SF, Garcia JG. Transactivation of sphingosine 1-phosphate receptors is essential for vascular barrier regulation: novel role for hyaluronan and CD44 receptor family. J Biol Chem. 2006; 281:34381–93. [PubMed: 16963454]
63. Zeng Y, Waters M, Andrews A, Honarmandi P, Ebong E, et al. Fluid shear stress induces the clustering of heparan sulfate via mobility of glypican-1 in lipid rafts. Am J Physiol Heart Circ Physiol. 2013; 305:H811–20. [PubMed: 23851278]
64. Florian JA, Kosky JR, Ainslie K, Pang Z, Dull RO, Tarbell JM. Heparan sulfate proteoglycan is a mechanosensor on endothelial cells. Circ Res. 2003; 93:e136–42. [PubMed: 14563712]
65. Pohl U, Herlan K, Huang A, Bassenge E. EDRF-mediated shear-induced dilation opposes myogenic vasoconstriction in small rabbit arteries. Am J Physiol. 1991; 261:H2016–23. [PubMed: 1721502]
66. Hecker M, Mulsch A, Bassenge E, Busse R. Vasoconstriction and increased flow: two principal mechanisms of shear stress-dependent endothelial autacoid release. Am J Physiol. 1993; 265:H828–33. [PubMed: 8105699]
67. Mochizuki S, Vink H, Hiramatsu O, Kajita T, Shigeto F, et al. Role of hyaluronic acid glycosaminoglycans in shear-induced endothelium-derived nitric oxide release. Am J Physiol Heart Circ Physiol. 2003; 285:H722–26. [PubMed: 12730059]
68. Nagy N, Freudenberger T, Melchior-Becker A, Rock K, Ter Braak M, et al. Inhibition of hyaluronan synthesis accelerates murine atherosclerosis: novel insights into the role of hyaluronan synthesis. Circulation. 2010; 122:2313–22. [PubMed: 21098434]
69. Rubio R, Ceballos G. Role of the endothelial glycocalyx in dromotropic, inotropic, and arrythmogenic effects of coronary flow. Am J Physiol Heart Circ Physiol. 2000; 278:H106–16. [PubMed: 10644590]
70. Pahakis MY, Kosky JR, Dull RO, Tarbell JM. The role of endothelial glycocalyx components in mechanotransduction of fluid shear stress. Biochem Biophys Res Commun. 2007; 355:228–33. [PubMed: 17291452]
71. Remuzzi A, Dewey CF Jr, Davies PF, Gimbrone MA Jr. Orientation of endothelial cells in shear fields in vitro. Biorheology. 1984; 21:617–30. [PubMed: 6487771]
72. Langille BL, Adamson SL. Relationship between blood flow direction and endothelial cell orientation at arterial branch sites in rabbits and mice. Circ Res. 1981; 48:481–88. [PubMed: 7460219]
73. Thi MM, Tarbell JM, Weinbaum S, Spray DC. The role of the glycocalyx in reorganization of the actin cytoskeleton under fluid shear stress: a “bumper-car” model. Proc Natl Acad Sci USA. 2004; 101:16483–88. [PubMed: 15545600]
74. Moon JJ, Matsumoto M, Patel S, Lee L, Guan JL, Li S. Role of cell surface heparan sulfate proteoglycans in endothelial cell migration and mechanotransduction. J Cell Physiol. 2005; 203:166–76. [PubMed: 15389626]

75. Yao Y, Rabodzey A, Dewey CF Jr. Glycocalyx modulates the motility and proliferative response of vascular endothelium to fluid shear stress. Am J Physiol Heart Circ Physiol. 2007; 293:H1023–30. [PubMed: 17468337]
76. Curry FR, Adamson RH. Vascular permeability modulation at the cell, microvessel, or whole organ level: towards closing gaps in our knowledge. Cardiovasc Res. 2010; 87:218–29. [PubMed: 20418473]
77. Dull RO, Dinavahi R, Schwartz L, Humphries DE, Berry D, et al. Lung endothelial heparan sulfates mediate cationic peptide-induced barrier dysfunction: a new role for the glycocalyx. Am J Physiol Lung Cell Mol Physiol. 2003; 285:L986–95. [PubMed: 12754183]
78. Weinbaum S, Zhang X, Han Y, Vink H, Cowin SC. Mechanotransduction and flow across the endothelial glycocalyx. Proc Natl Acad Sci USA. 2003; 100:7988–95. [PubMed: 12810946]
79. Ebong EE, Lopez-Quintero SV, Rizzo V, Spray DC, Tarbell JM. Shear-induced endothelial NOS activation and remodeling via heparan sulfate, glypican-1, and syndecan-1. Integr Biol. 2014; 6:338–47.
80. Belting M. Heparan sulfate proteoglycan as a plasma membrane carrier. Trends Biochem Sci. 2003; 28:145–51. [PubMed: 12633994]
81. Bevan JA, Siegel G. Blood vessel wall matrix flow sensor: evidence and speculation. Blood Vessels. 1991; 28:552–56. [PubMed: 1782412]
82. Hileman RE, Fromm JR, Weiler JM, Linhardt RJ. Glycosaminoglycan-protein interactions: definition of consensus sites in glycosaminoglycan binding proteins. Bioessays. 1998; 20:156–67. [PubMed: 9631661]
83. Bishop JR, Schuksz M, Esko JD. Heparan sulphate proteoglycans fine-tune mammalian physiology. Nature. 2007; 446:1030–37. [PubMed: 17460664]
84. Conway D, Schwartz MA. Lessons from the endothelial junctional mechanosensory complex. F1000 Biol Rep. 2012; 4:1. [PubMed: 22238515]
85. Osawa M, Masuda M, Kusano K, Fujiwara K. Evidence for a role of platelet endothelial cell adhesion molecule-1 in endothelial cell mechanosignal transduction: Is it a mechanoresponsive molecule? J Cell Biol. 2002; 158:773–85. [PubMed: 12177047]
86. Chiu YJ, McBeath E, Fujiwara K. Mechanotransduction in an extracted cell model: Fyn drives stretch- and flow-elicited PECAM-1 phosphorylation. J Cell Biol. 2008; 182:753–63. [PubMed: 18710921]
87. Collins C, Guilluy C, Welch C, O'Brien ET, Hahn K, et al. Localized tensional forces on PECAM-1 elicit a global mechanotransduction response via the integrin-RhoA pathway. Curr Biol. 2012; 22:2087–94. [PubMed: 23084990]
88. Dela Paz NG, Melchior B, Shayo FY, Frangos JA. Heparan sulfates mediate the interaction between platelet endothelial cell adhesion molecule-1 (PECAM-1) and the $G\alpha_{q/11}$ subunits of heterotrimeric G proteins. J Biol Chem. 2014; 289(11):7413–24. [PubMed: 24497640]
89. Garin G, Berk BC. Flow-mediated signaling modulates endothelial cell phenotype. Endothelium. 2006; 13:375–84. [PubMed: 17169770]
90. Giddens DP, Zarins CK, Glagov S. The role of fluid mechanics in the localization and detection of atherosclerosis. J Biomech Eng. 1993; 115:588–94. [PubMed: 8302046]
91. Tedgui A, Mallat Z. Anti-inflammatory mechanisms in the vascular wall. Circ Res. 2001; 88:877–87. [PubMed: 11348996]
92. Tsou JK, Gower RM, Ting HJ, Schaff UY, Insana MF, et al. Spatial regulation of inflammation by human aortic endothelial cells in a linear gradient of shear stress. Microcirculation. 2008; 15:311–23. [PubMed: 18464160]
93. Libby P. Inflammation in atherosclerosis. Arterioscler Thromb Vasc Biol. 2012; 32:2045–51. [PubMed: 22895665]
94. Davies PF, Civelek M, Fang Y, Guerraty MA, Passerini AG. Endothelial heterogeneity associated with regional athero-susceptibility and adaptation to disturbed blood flow in vivo. Semin Thromb Hemost. 2010; 36:265–75. [PubMed: 20533180]
95. Sun C, Alkhoury K, Wang YI, Foster GA, Radecke CE, et al. IRF-1 and miRNA126 modulate VCAM-1 expression in response to a high-fat meal. Circ Res. 2012; 111:1054–64. [PubMed: 22874466]

96. Arisaka T, Mitsumata M, Kawasumi M, Tohjima T, Hirose S, et al. Effects of shear stress on glycosaminoglycan synthesis in vascular endothelial cells. Ann NY Acad Sci. 1995; 748:543–54. [PubMed: 7695202]

97. Simon SI, Nyunt T, Florine-Casteel K, Ritchie K, Ting-Beall HP, et al. Dynamics of neutrophil membrane compliance and microstructure probed with a micropipet-based piconewton force transducer. Ann Biomed Eng. 2007; 35:595–604. [PubMed: 17370125]

98. Rehm M, Bruegger D, Christ F, Conzen P, Thiel M, et al. Shedding of the endothelial glycocalyx in patients undergoing major vascular surgery with global and regional ischemia. Circulation. 2007; 116:1896–906. [PubMed: 17923576]

99. Chiu JJ, Chen LJ, Lee PL, Lee CI, Lo LW, et al. Shear stress inhibits adhesion molecule expression in vascular endothelial cells induced by coculture with smooth muscle cells. Blood. 2003; 101:2667–74. [PubMed: 12468429]

100. Chiu JJ, Lee PL, Chen CN, Lee CI, Chang SF, et al. Shear stress increases ICAM-1 and decreases VCAM-1 and E-selectin expressions induced by tumor necrosis factor-α in endothelial cells. Arterioscler Thromb Vasc Biol. 2004; 24:73–79. [PubMed: 14615388]

101. Tsao PS, Buitrago R, Chan JR, Cooke JP. Fluid flow inhibits endothelial adhesiveness: nitric oxide and transcriptional regulation of VCAM-1. Circulation. 1996; 94:1682–89. [PubMed: 8840861]

102. Tsuboi H, Ando J, Korenaga R, Takada Y, Kamiya A. Flow stimulates ICAM-1 expression time and shear stress dependently in cultured human endothelial cells. Biochem Biophys Res Commun. 1995; 206:988–96. [PubMed: 7832815]

103. Curry FR, Adamson RH. Tonic regulation of vascular permeability. Acta Physiol (Oxf). 2013; 207:628–49. [PubMed: 23374222]

104. Bode C, Sensken SC, Peest U, Beutel G, Thol F, et al. Erythrocytes serve as a reservoir for cellular and extracellular sphingosine 1-phosphate. J Cell Biochem. 2010; 109:1232–43. [PubMed: 20186882]

105. Venkataraman K, Lee YM, Michaud J, Thangada S, Ai Y, et al. Vascular endothelium as a contributor of plasma sphingosine 1-phosphate. Circ Res. 2008; 102:669–76. [PubMed: 18258856]

106. Hanel P, Andreani P, Graler MH. Erythrocytes store and release sphingosine 1-phosphate in blood. FASEB J. 2007; 21:1202–9. [PubMed: 17215483]

107. Kobayashi N, Yamaguchi A, Nishi T. Characterization of the ATP-dependent sphingosine 1-phosphate transporter in rat erythrocytes. J Biol Chem. 2009; 284:21192–200. [PubMed: 19531471]

108. Camerer E, Regard JB, Cornelissen I, Srinivasan Y, Duong DN, et al. Sphingosine-1-phosphate in the plasma compartment regulates basal and inflammation-induced vascular leak in mice. J Clin Investig. 2009; 119:1871–79. [PubMed: 19603543]

109. Christoffersen C, Nielsen LB. Apolipoprotein M: bridging HDL and endothelial function. Curr Opin Lipidol. 2013; 24:295–300. [PubMed: 23652568]

110. Ho-Tin-Noé B, Demers M, Wagner DD. How platelets safeguard vascular integrity. J Thromb Haemost. 2011; 9(Suppl 1):56–65. [PubMed: 21781242]

111. Stokes KY, Granger DN. Platelets: a critical link between inflammation and microvascular dysfunction. J Physiol. 2012; 590:1023–34. [PubMed: 22183721]

112. Wang L, Dudek SM. Regulation of vascular permeability by sphingosine 1-phosphate. Microvasc Res. 2009; 77:39–45. [PubMed: 18973762]

113. Adamson RH, Sarai RK, Clark JF, Altangerel A, Thirkill TL, Curry FE. Attenuation by sphingosine-1-phosphate of rat microvessel acute permeability response to bradykinin is rapidly reversible. Am J Physiol Heart Circ Physiol. 2012; 302:H1929–35. [PubMed: 22427519]

114. Adamson RH, Sarai RK, Altangerel A, Clark JF, Weinbaum S, Curry FE. Microvascular permeability to water is independent of shear stress, but dependent on flow direction. Am J Physiol Heart Circ Physiol. 2013; 304:H1077–84. [PubMed: 23417864]

115. Nitz T, Eisenblatter T, Psathaki K, Galla HJ. Serum-derived factors weaken the barrier properties of cultured porcine brain capillary endothelial cells in vitro. Brain Res. 2003; 981:30–40. [PubMed: 12885423]

116. Curry FE, Clark JF, Adamson RH. Erythrocyte-derived sphingosine-1-phosphate stabilizes basal hydraulic conductivity and solute permeability in rat microvessels. Am J Physiol Heart Circ Physiol. 2012; 303:H825–34. [PubMed: 22865384]
117. Kendall S, Michel CC. The measurement of permeability in single rat venules using the red cell microperfusion technique. Exp Physiol. 1995; 80:359–72. [PubMed: 7640005]
118. Neal CR, Bates DO. Measurement of hydraulic conductivity of single perfused *Rana* mesenteric microvessels between periods of controlled shear stress. J Physiol. 2002; 543:947–57. [PubMed: 12231650]
119. Kajimura M, Michel CC. Flow modulates the transport of K^+ through the walls of single perfused mesenteric venules in anaesthetised rats. J Physiol. 1999; 521:665–77. [PubMed: 10601497]
120. Kim MH, Harris NR, Tarbell JM. Regulation of capillary hydraulic conductivity in response to an acute change in shear. Am J Physiol Heart Circ Physiol. 2005; 289:H2126–35. [PubMed: 15994851]
121. Tarbell JM. Shear stress and the endothelial transport barrier. Cardiovasc Res. 2010; 87:320–30. [PubMed: 20543206]
122. Yuan Y, Granger HJ, Zawieja DC, Chilian WM. Flow modulates coronary venular permeability by a nitric oxide-related mechanism. Am J Physiol. 1992; 263:H641–46. [PubMed: 1510161]
123. Huxley VH, Wang JJ, Sarelius IH. Adaptation of coronary microvascular exchange in arterioles and venules to exercise training and a role for sex in determining permeability responses. Am J Physiol Heart Circ Physiol. 2007; 293:H1196–205. [PubMed: 17434979]
124. Huxley VH, Williams DA. Basal and adenosine-mediated protein flux from isolated coronary arterioles. Am J Physiol. 1996; 271:H1099–108. [PubMed: 8853347]
125. Yamawaki H, Lehoux S, Berk BC. Chronic physiological shear stress inhibits tumor necrosis factor-induced proinflammatory responses in rabbit aorta perfused ex vivo. Circulation. 2003; 108:1619–25. [PubMed: 12963644]
126. Fernández-Pisonero I, Dueñas AI, Barreiro O, Montero O, Sánchez-Madrid F, García-Rodríguez C. Lipopolysaccharide and sphingosine-1-phosphate cooperate to induce inflammatory molecules and leukocyte adhesion in endothelial cells. J Immunol. 2012; 189:5402–10. [PubMed: 23089395]
127. Liu Y, Collins C, Kiosses WB, Murray AM, Joshi M, et al. A novel pathway spatiotemporally activates Rac1 and redox signaling in response to fluid shear stress. J Cell Biol. 2013; 201:863–73. [PubMed: 23733346]
128. Cyster JG, Schwab SR. Sphingosine-1-phosphate and lymphocyte egress from lymphoid organs. Annu Rev Immunol. 2012; 30:69–94. [PubMed: 22149932]
129. Fyrst H, Saba JD. An update on sphingosine-1-phosphate and other sphingolipid mediators. Nat Chem Biol. 2010; 6:489–97. [PubMed: 20559316]
130. Hla T. Physiological and pathological actions of sphingosine 1-phosphate. Semin Cell Dev Biol. 2004; 15:513–20. [PubMed: 15271296]
131. Jung B, Obinata H, Galvani S, Mendelson K, Ding BS, et al. Flow-regulated endothelial S1P receptor-1 signaling sustains vascular development. Dev Cell. 2012; 23:600–10. [PubMed: 22975328]
132. Lewis JC, Taylor RG, Jones ND, St Clair RW, Cornhill JF. Endothelial surface characteristics in pigeon coronary artery atherosclerosis. I Cellular alterations during the initial stages of dietary cholesterol challenge. Lab Investig. 1982; 46:123–38. [PubMed: 7062718]
133. Brower JB, Targovnik JH, Caplan MR, Massia SP. High glucose-mediated loss of cell surface heparan sulfate proteoglycan impairs the endothelial shear stress response. Cytoskeleton (Hoboken). 2010; 67:135–41. [PubMed: 20217676]
134. Lopez-Quintero SV, Cancel LM, Pierides A, Antonetti D, Spray DC, Tarbell JM. High glucose attenuates shear-induced changes in endothelial hydraulic conductivity by degrading the glycocalyx. PLoS ONE. 2013; 8(11):e78954. [PubMed: 24260138]
135. Danese C, Vestri AR, D'Alfonso V, Deriu G, Dispensa S, et al. Do hypertension and diabetes mellitus influence the site of atherosclerotic plaques? Clin Ter. 2006; 157:9–13. [PubMed: 16669546]

136. Reyes-Soffer G, Holleran S, Di Tullio MR, Homma S, Boden-Albala B, et al. Endothelial function in individuals with coronary artery disease with and without type 2 diabetes mellitus. Metabolism. 2010; 59:1365–71. [PubMed: 20102776]

137. Vlahu CA, Lemkes BA, Struijk DG, Koopman MG, Krediet RT, Vink H. Damage of the endothelial glycocalyx in dialysis patients. J Am Soc Nephrol. 2012; 23:1900–8. [PubMed: 23085635]

138. Salmon AH, Satchell SC. Endothelial glycocalyx dysfunction in disease: albuminuria and increased microvascular permeability. J Pathol. 2012; 226:562–74. [PubMed: 22102407]

139. Luft JH. Fine structures of capillary and endocapillary layer as revealed by ruthenium red. Fed Proc. 1966; 25:1773–83. [PubMed: 5927412]

140. Potter DR, Damiano ER. The hydrodynamically relevant endothelial cell glycocalyx observed in vivo is absent in vitro. Circ Res. 2008; 102:770–76. [PubMed: 18258858]

141. Devaraj S, Yun JM, Adamson G, Galvez J, Jialal I. C-reactive protein impairs the endothelial glycocalyx resulting in endothelial dysfunction. Cardiovasc Res. 2009; 84:479–84. [PubMed: 19620133]

142. Chappell D, Jacob M, Paul O, Rehm M, Welsch U, et al. The glycocalyx of the human umbilical vein endothelial cell: an impressive structure ex vivo but not in culture. Circ Res. 2009; 104:1313–17. [PubMed: 19423849]

143. Van Haaren PM, VanBavel E, Vink H, Spaan JA. Localization of the permeability barrier to solutes in isolated arteries by confocal microscopy. Am J Physiol Heart Circ Physiol. 2003; 285:H2848–56. [PubMed: 12907418]

144. Janczyk P, Hansen S, Bahramsoltani M, Plendl J. The glycocalyx of human, bovine and murine microvascular endothelial cells cultured in vitro. J Electron Microsc. 2010; 59:291–98.

145. Ueda A, Shimomura M, Ikeda M, Yamaguchi R, Tanishita K. Effect of glycocalyx on shear-dependent albumin uptake in endothelial cells. Am J Physiol Heart Circ Physiol. 2004; 287:H2287–94. [PubMed: 15256377]

146. Singh A, Satchell SC, Neal CR, McKenzie EA, Tooke JE, Mathieson PW. Glomerular endothelial glycocalyx constitutes a barrier to protein permeability. J Am Soc Nephrol. 2007; 18:2885–93. [PubMed: 17942961]

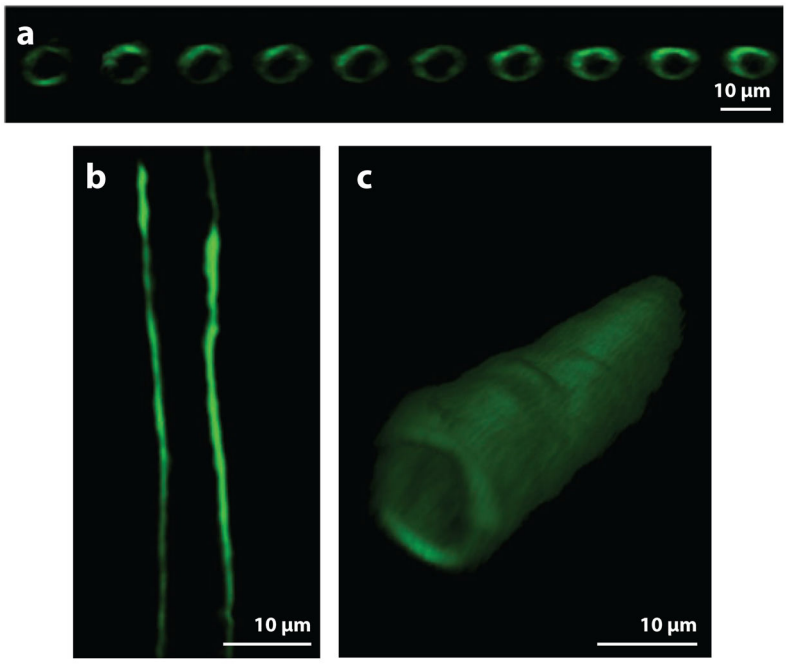

Figure 1.

The glycocalyx on the surface of a capillary in the rat mesentery labeled with antiheparan sulfate antibody and imaged by laser-scanning confocal microscopy. Images of the glycocalyx (*a*) in a longitudinal series of cross sections, (*b*) in a centerline longitudinal section, and (*c*) in a three-dimensional reconstruction. (Figure adapted with permission from 41.)

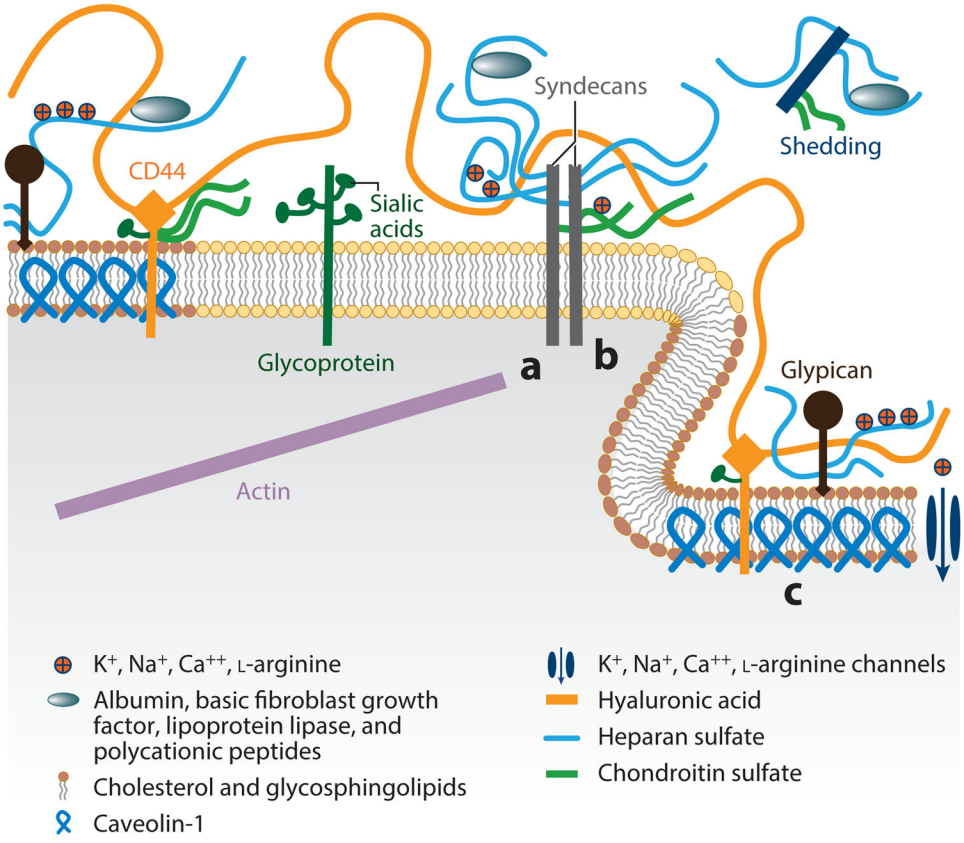

Figure 2.

Schematic diagram showing the components and spatial organization of the endothelial glycocalyx. In the diagram, *a* denotes the region where the cytoplasmic tail of syndecan links to the actin cytoskeleton, *b* indicates oligomerization of syndecans, and *c* labels caveolin protein within a caveola. All other components are labeled in the diagram. (Figure adapted with permission from 11.)

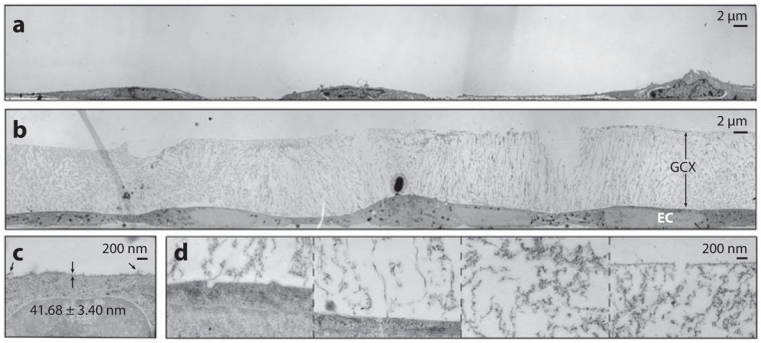

Figure 3.

TEM of GCX-covered BAECs (*a*) preserved conventionally, labeled with ruthenium red and osmium tetroxide, and alcohol dehydrated and (*b*) preserved by cryo-EM and osmium tetroxide stained. (*c*) High-magnification image of a conventionally preserved BAEC GCX. Arrows indicate extended strands of GCX. (*d*) High-magnification image of a cryo-EM BAEC GCX, showing (*from left to right*) locations near the cell membrane, farther away from the cell membrane, in the center region of the GCX, and at the most apical surface of the GCX. Abbreviations: BAECs, bovine aortic endothelial cells; EM, electron microscopy; GCX, glycocalyx; TEM, transmission electron microscopy. (Figure adapted with permission from 33.)

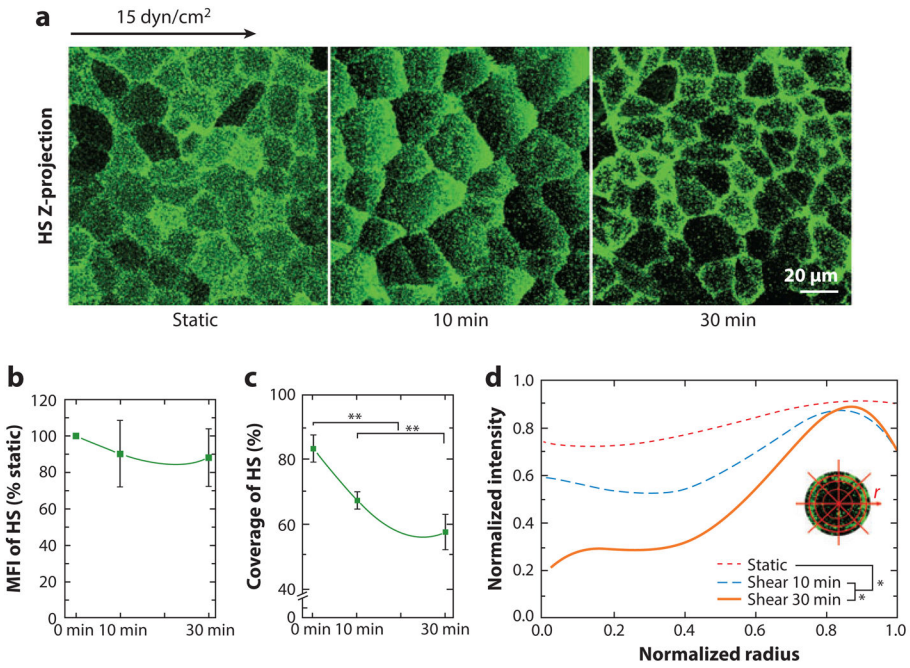

Figure 4.

Redistribution of heparan sulfate (HS) under shear stress. (*a*) Representative immunofluorescent images of an HS-labeled rat fat pad endothelial cell (RFPEC) under static and shear stress conditions. Respective changes in the (*b*) mean fluorescence intensity (MFI), (*c*) coverage, and (*d*) average radial profile of HS. The zero-radius represents the center of the cell. Significant difference: $^{*}P < 0.05$; $^{**}P < 0.01$. (Figure adapted with permission from 63.)

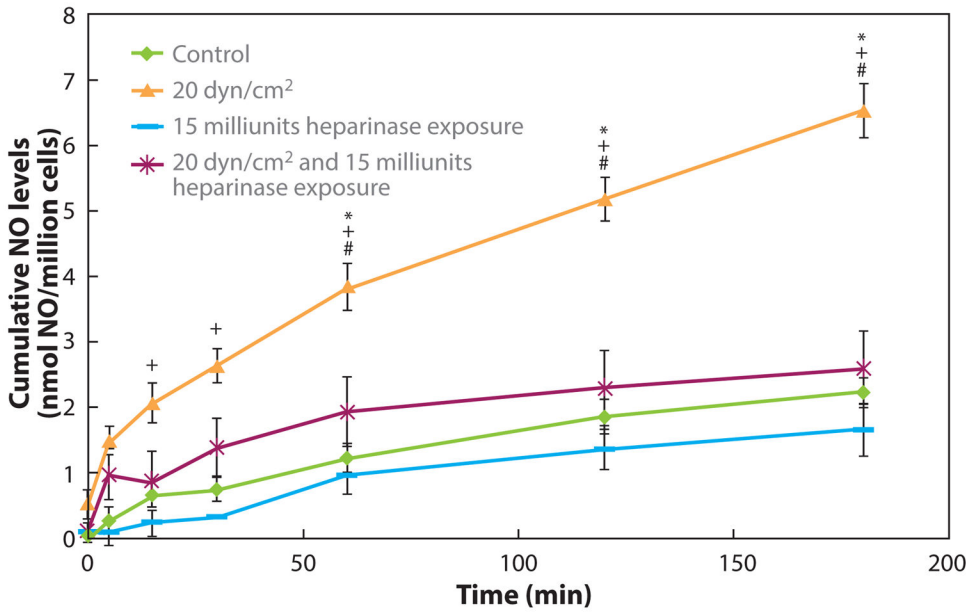

Figure 5.

The GCX mediates NO production in response to shear stress. Bovine aortic ECs were exposed to a step increase in shear stress from static to 20 dyn/cm^2 at time 0 in a parallel-plate flow chamber. The HS GAG component was either partially removed by a heparinase enzyme treatment or left intact, and NO released into the media was monitored over time. Shear-induced NO production was completely blocked by the enzyme treatment. Abbreviations: GAG, glycosaminoglycan; GCX, glycocalyx; HS, heparan sulfate; NO, nitric oxide. (Figure adapted with permission from 64.)

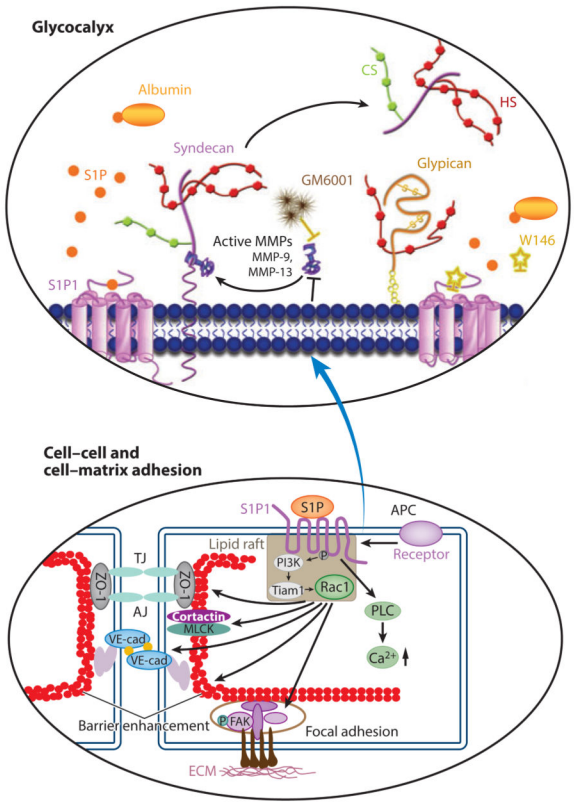

Figure 6.

S1P-activated pathways that regulate (*a*) the stability of the glycocalyx by regulating MMP release (*top*) and (*b*) the interendothelial junctions and adhesion to the basement membrane (*bottom*). For both panels, signaling involves ligation of S1P to S1P1 to stimulate Rac1 activation. In the top panel, serum albumin and HDL carry S1P that activates S1P1. The activation of S1P1 inhibits the activity of MMPs. The S1P1 agonist activity can be blocked by the receptor antagonist W146. After the bound S1P on the cell surface is cleared by removal of albumin (or S1P), the inhibition of MMP activity (MMP-9 and -13) is attenuated, and this induces the shedding of syndecan-1 by cleaving its ectodomain. The glycocalyx is protected when MMP activity is inhibited. The specific pathways leading control of MMP release in the top panel have not been investigated in as much detail as those that regulate the interendothelial junctions shown in the bottom panel (see 29). In the bottom panel, activation of Rac1 induces AJ and TJ assembly, cytoskeletal reorganization, and formation of focal adhesions that combine to enhance vascular barrier function. Other S1P-dependent mechanisms include an increase in intracellular Ca^{2+} concentration and transactivation of S1P1 signaling by other barrier-enhancing agents. Abbreviations: AJ, adherens junction; APC, activated protein C signaling through the thrombin receptor; CS, chondroitin sulfate; ECM, extracellular matrix; FAK, focal adhesion kinase; HDL, high-density lipoprotein; HS, heparan sulfate; MLCK, endothelial myosin light chain kinase; MMPs, matrix metalloproteinases; P, phosphorylated focal adhesion kinase; PI3K, phosphoinositide 3-kinase; PLC, phospholipase C; Rac1, a Rho family GTPase; S1P, sphingosine-1-phosphate; S1P1, sphingosine-1-phosphate receptor 1; Tiam1, T-cell lymphoma invasion and metastasis

gene 1; TJ, tight junction; VE-cad, vascular endothelial cadherin; ZO-1, zona occludens-1. (See text for more details; figure adapted with permission from 99 and 30.)

Table 1

Representative values of GCX thickness derived from a variety of techniques (adapted from 33)

Setting(s)	Microscopic visualization	GCX fixation	GCX marker(s)	Species and vessel/cell type	GCX thickness (μm)	Reference
In vivo and ex vivo	TEM	Glut	RR	Mouse diaphragmatic capillary	0.02	139
	TEM	Glut	Fluorocarbon	Rat capillary	0.05–0.10	34
	IM	No fixation	FITC dextran-labeled plasma	Hamster muscle capillary[a]	0.40–0.50	35
	μ-PIV	No fixation	Fluorescent microspheres in saline	Mouse cremaster venules[b]	0.50	140
	TEM	Glut/PFA	Alcian blue and lanthanum	Rat aorta	0.53	141
	TEM	Glut	Lanthanum	HUVEC	0.80	142
	IM	No fixation	FITC dextran-labeled plasma	Rat small arteries[c]	2.00–3.00	143
	TPLSM	No fixation	WGA-FITC	Mouse carotid arteries	4.50	44
	CLSM	No fixation	Anti-HS tagged with HABP-AF555 and -AF488	Mouse carotid arteries	2.20–4.30	46
In vitro	TEM	Glut	RR	MCMVEC	0.00–0.20	144
	TEM	Glut	RR	HDMVEC	0.01–0.02	144
	TEM	Glut	RR	BLMVEC	0.01–0.03	144
	μ-PIV	No fixation	Fluorescent microspheres in media	HUVEC[d]	0.03	140
	μ-PIV	No fixation	Fluorescent microspheres in media	BAEC[e]	0.02	140
	TEM	Glut	Lanthanum	HUVEC	0.03	142
	TEM	Glut	RR	BAEC	0.02–0.04	145
	TEM	Glut	Alcian blue	CiGEnC	0.20	146
	TEM	Glut/PFA	Alcian blue and lanthanum	HAEC	0.85	141
	CLSM	PFA	Fluorescent anti-HS	RFPEC	2.00[f]	73
	CLSM	No fixation	WGA-FITC	HUVEC	2.50	39
	CLSM	PFA	HABP-FITC and fluorescent anti-HS	BLMVEC	2.00–3.00	40

Abbreviations: μ-PIV, microparticle image velocimetry; AF555, Alexa Fluor 555; AF488, Alexa Fluor 488; BAEC, bovine aortic EC; BLMVEC, bovine lung microvascular EC; BLMVEC, bovine luteal microvascular EC; CiGEnC, conditionally immortalized human glomerular EC; CLSM, confocal laser scanning microscopy; EC, endothelial cells; FITC, fluorescein isothiocyanate; glut, glutaraldehyde; HABP, hyaluronic acid–binding protein; HAEC, human aortic ECs; HDMVEC, human dermal microvascular EC; HS, heparan sulfate; HUVEC, human umbilical vein EC; IM, intravital microscopy; MCMVEC, murine cardiac microvascular EC; PFA, paraformaldehyde; RFPEC, rat fat pad EC; RR, ruthenium red; TEM, transmission electron microscopy; TPLSM, two-photon laser scanning microscopy; WGA, wheat germ agglutinin.

[a] 5.1 ± 0.1 μm diameter.

[b] 45 ± 20 μm diameter.

[c] 148 ± 5 μm diameter.

[d] Cells were plated in collagen channels of ~110–150-μm diameter.

[e] Cells were plated in collagen channels of ~88–109-μm diameter.

[f] GCX thickness was not reported in the publication but was obtained in reference to the scale bar and relative to the cell dimensions.